Tropical wave theory, 1

Imagine the atmosphere has a rigid lid at the tropopause, $z = H$. (This is **not true**, but for some purposes is an adequate approximation.) Then there will be vertical modes. For simplicity assume a Boussinesq atmosphere. Since $w = 0$ at surface and lid, the modes must look like (for constant stratification)

$$w \sim \sin(\frac{n\pi z}{H}).$$

Since the temperature equation (linearized) looks like

$$\frac{\partial T}{\partial t} + wN^2 = Q_c + Q_R,$$

T must have the same vertical structure as w, peaking in mid-troposphere.

By mass conservation then we will have $u,\ v \sim \cos(\frac{n\pi z}{H})$. For dry equations, convective heating is a "forcing" on the right-hand side. Observations often show a single peak in Q_c as a function of height, so we expect $n = 1$ to be important. However, stratiform heating will also drive an $n = 2$ component.

Tropical wave theory, 2

If Q_c is **given**, then we have a problem in dry dynamics to solve for the response. There is a large literature on this problem. We particularly study the linear, Boussinesq problem on the **equatorial β-plane**, where the Coriolis parameter is approximated by the first term in a Taylor expansion around the equator:

$$f = y\frac{df}{dy} = \beta y,$$

where

$$\beta = \frac{2\Omega \cos\lambda}{a},$$

y is distance from the equator (positive north), λ latitude in radians, a the radius of the earth.

Tropical wave theory, 3

Having assumed a single vertical mode, some imposed heating $Q(x, y, t)$, and linear damping, we can write the equations as

$$\frac{\partial u}{\partial t} - \beta y v = -\frac{\partial p}{\partial x} - \epsilon u$$
$$\frac{\partial v}{\partial t} + \beta y u = -\frac{\partial p}{\partial x} - \epsilon v$$
$$\frac{\partial p}{\partial t} + \frac{\partial u}{\partial x} + \frac{\partial v}{\partial y} = Q - \epsilon_T p$$

The last equation results from a combination of hydrostatic balance, mass conservation, and temperature equations. These are isomorphic to the (linear) shallow water equations on the equatorial β plane with a mass source and linear damping on mass and momentum.
Here ϵ_T can be thought of as radiative damping. These have been nondimensionalized by free gravity wave speed $c = NH/\pi$ for velocity, length by **equatorial deformation radius** $L_\beta = \sqrt{c/\beta}$, time by $L_\beta/c = 1/\sqrt{\beta c}$.

Tropical wave theory, 4

We can first study the **linear modes of the unforced, undamped system** (Matsuno, 1966):

$$\frac{\partial u}{\partial t} - \beta y v = -\frac{\partial p}{\partial x}$$
$$\frac{\partial v}{\partial t} + \beta y u = -\frac{\partial p}{\partial x}$$
$$\frac{\partial p}{\partial t} + \frac{\partial u}{\partial x} + \frac{\partial v}{\partial y} = 0$$

Tropical wave theory, 5

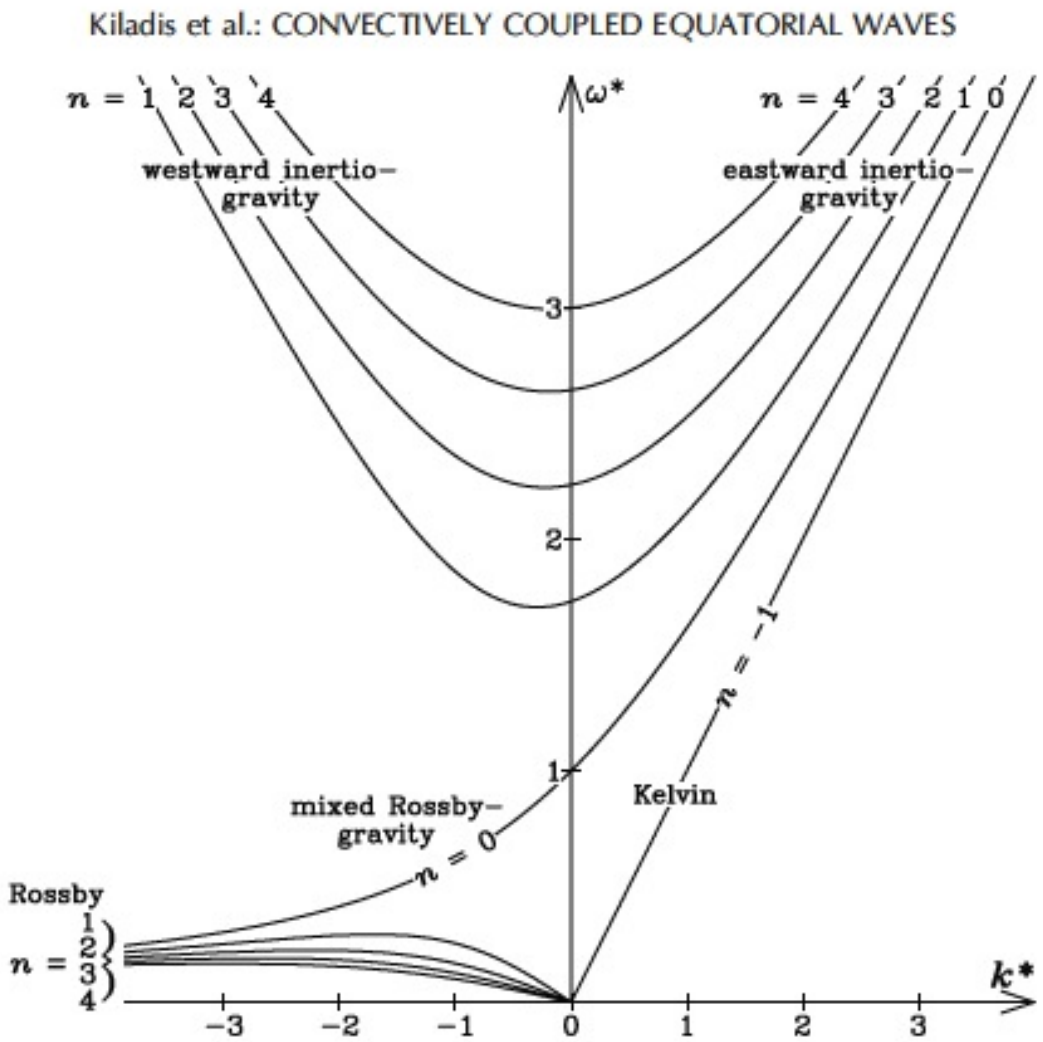

Kiladis et al., *Rev. Geopys.*, 2009 (following Matsuno, 1966, *J. Meteor. Soc. Japan*)

Tropical wave theory, 6

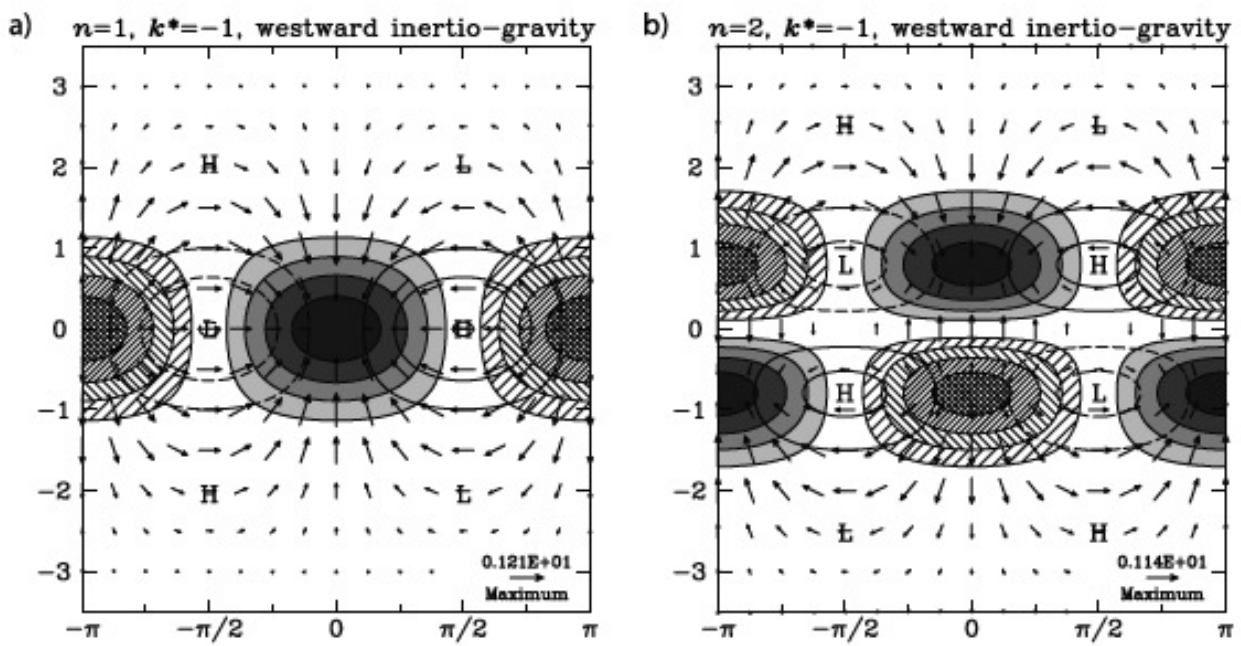

Kiladis et al., *Rev. Geopys.*, 2009 (following Matsuno, 1966, *J. Meteor. Soc. Japan*).

Tropical wave theory, 7

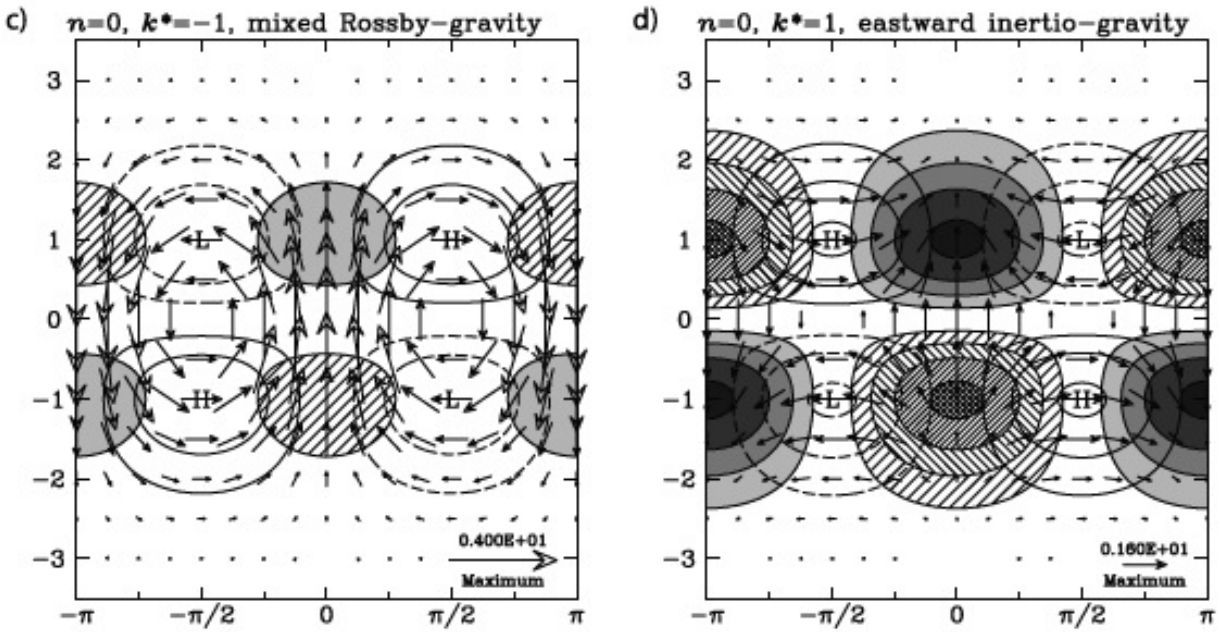

Kiladis et al., *Rev. Geopys.*, 2009 (following Matsuno, 1966, *J. Meteor. Soc. Japan*).

Tropical wave theory, 8

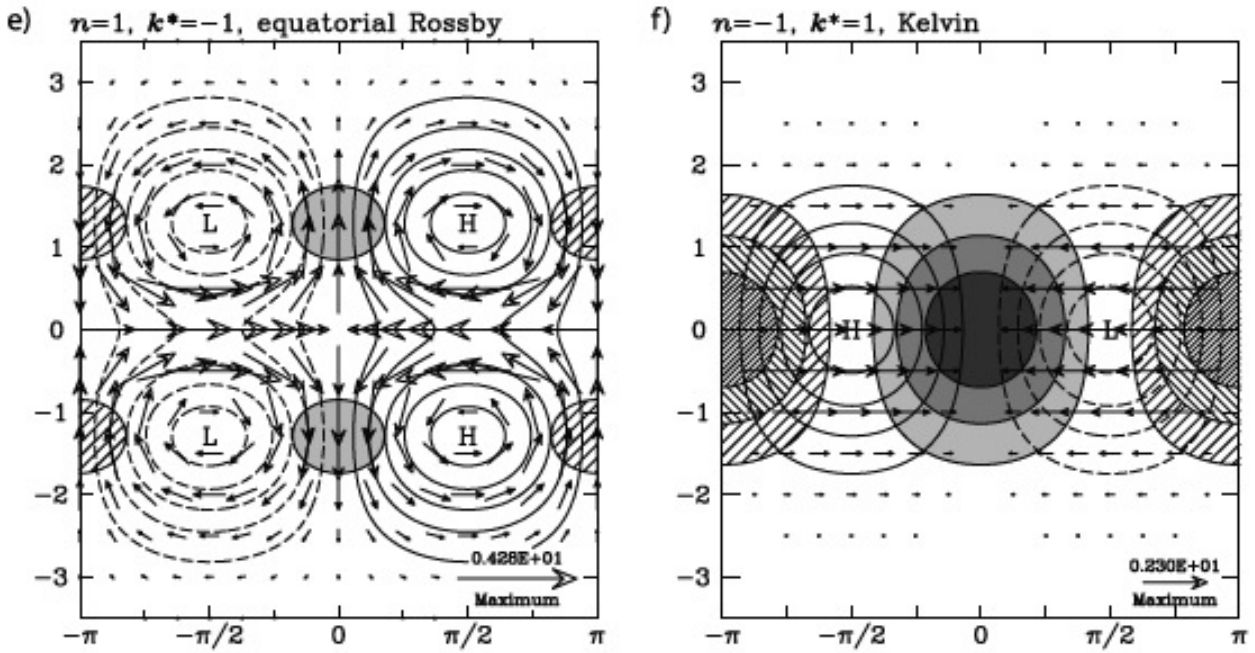

Kiladis et al., *Rev. Geopys.*, 2009 (following Matsuno, 1966, *J. Meteor. Soc. Japan*).

Slides on observed convectively coupled waves here.

Convectively coupled equatorial waves

Figures from Wheeler and Kiladis (1999) Wheeler et al. (2000), Sobel et al. (2004), Lau and Lau (1990), Reed and Recker (1971)

Adam Sobel, Columbia

FDEPS, Kyoto

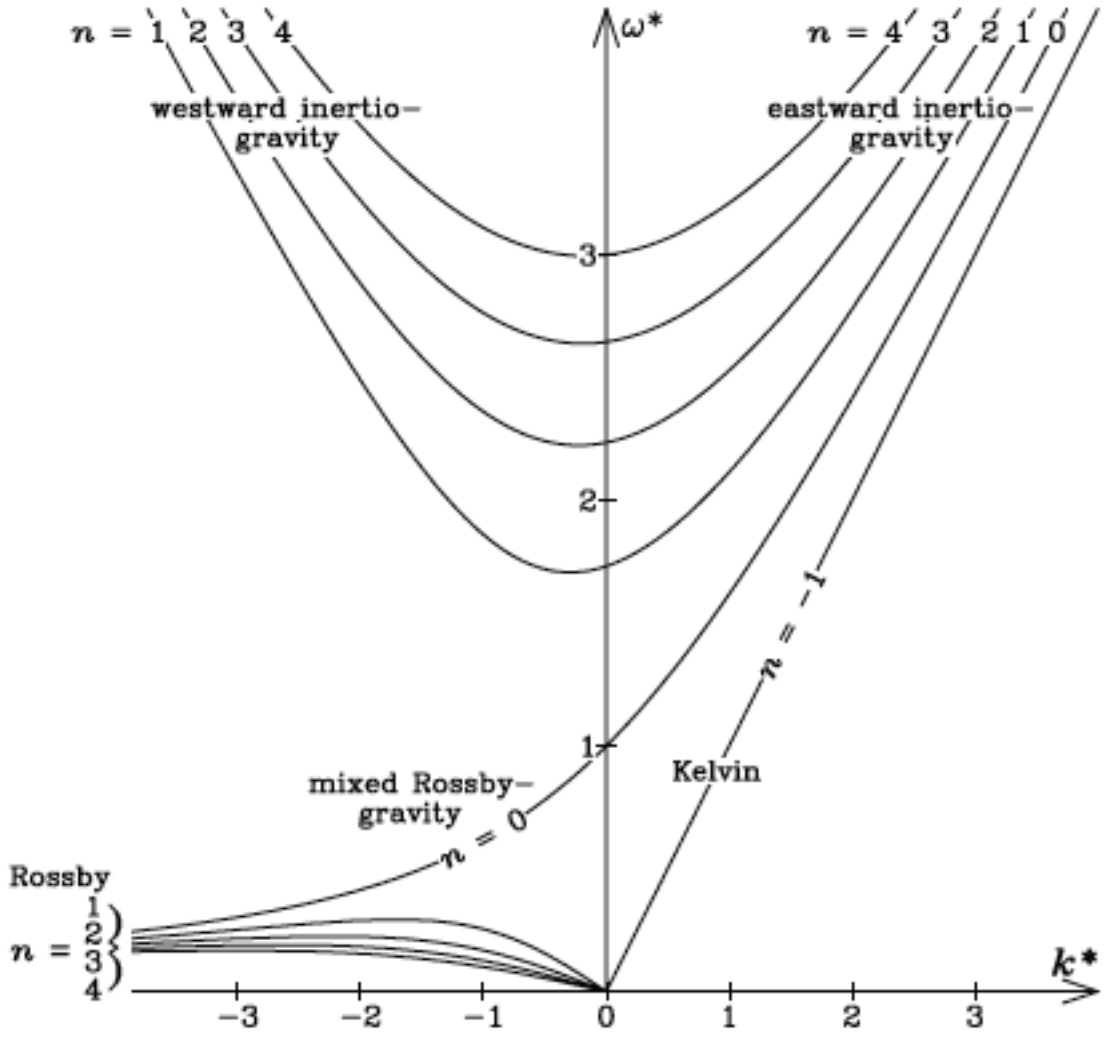
n = 1 2 3 4
ω*
n = 4′ 3′ 2′ 1′ 0′
westward inertio–
gravity
eastward inertio–
gravity
3
2
1
n = −1
mixed Rossby–
gravity
n = 0
Kelvin
Rossby
n = 1
2
3
4
k*
−3
−2
−1
0
1
2
3

Wave number – frequency power spectra of OLR, 15S-15N, equatorially symmetric and antisymmetric components

antisymmetric

symmetric

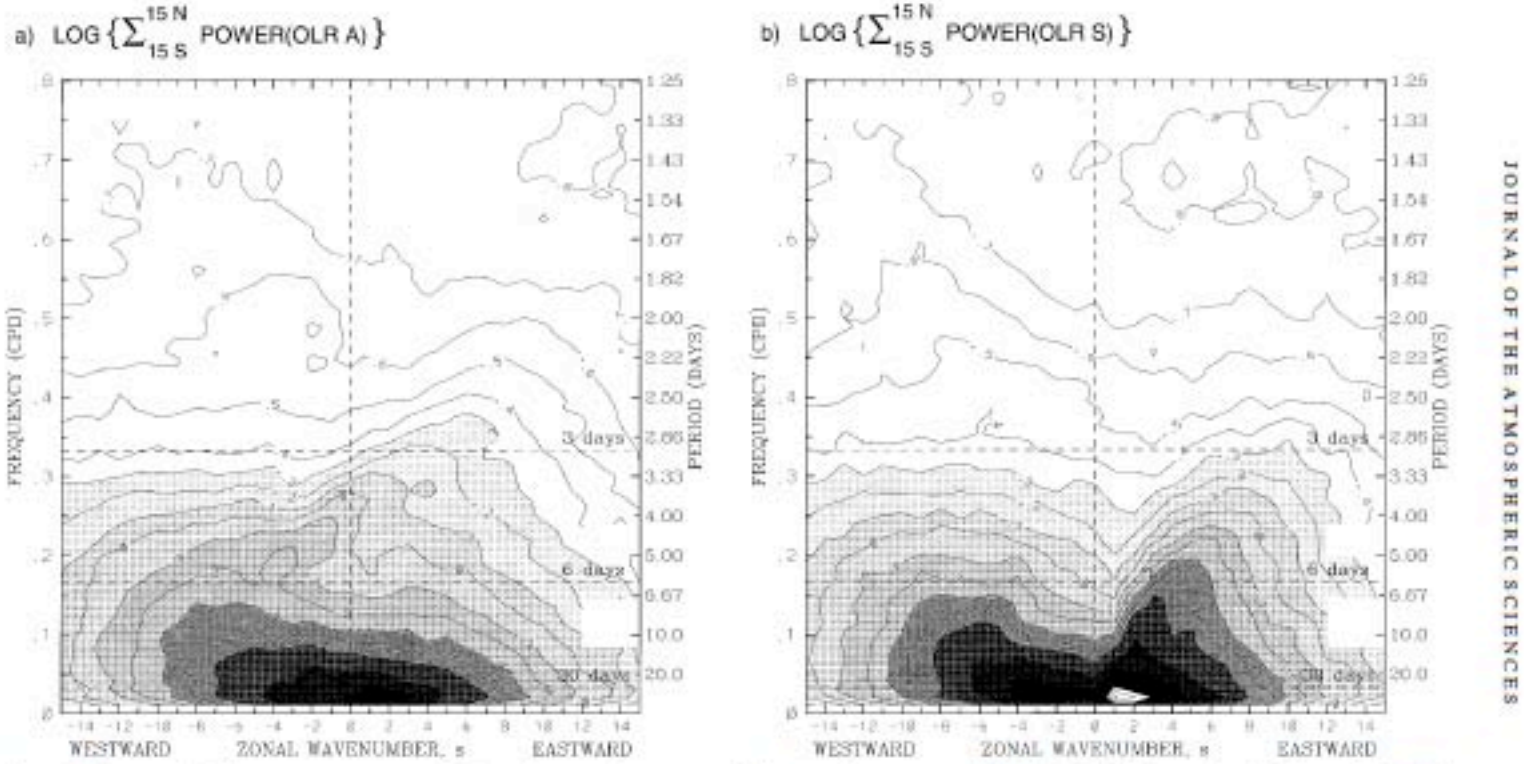

FIG. 1. Zonal wavenumber-frequency power spectra of the (a) antisymmetric component and (b) symmetric component of OLR, calculated for the entire period of record from 1979 to 1996. For both components, the power has been summed over 15°S–15°N lat, and the base-10 logarithm taken for plotting. Contour interval is 0.1 arbitrary units (see text). Shading is incremented in steps of 0.2. Certain erroneous spectral peaks from artifacts of the satellite sampling (see text) are not plotted.

"Background spectrum" – obtained by taking total spectrum (sym + anti-sym) and smoothing repeatedly

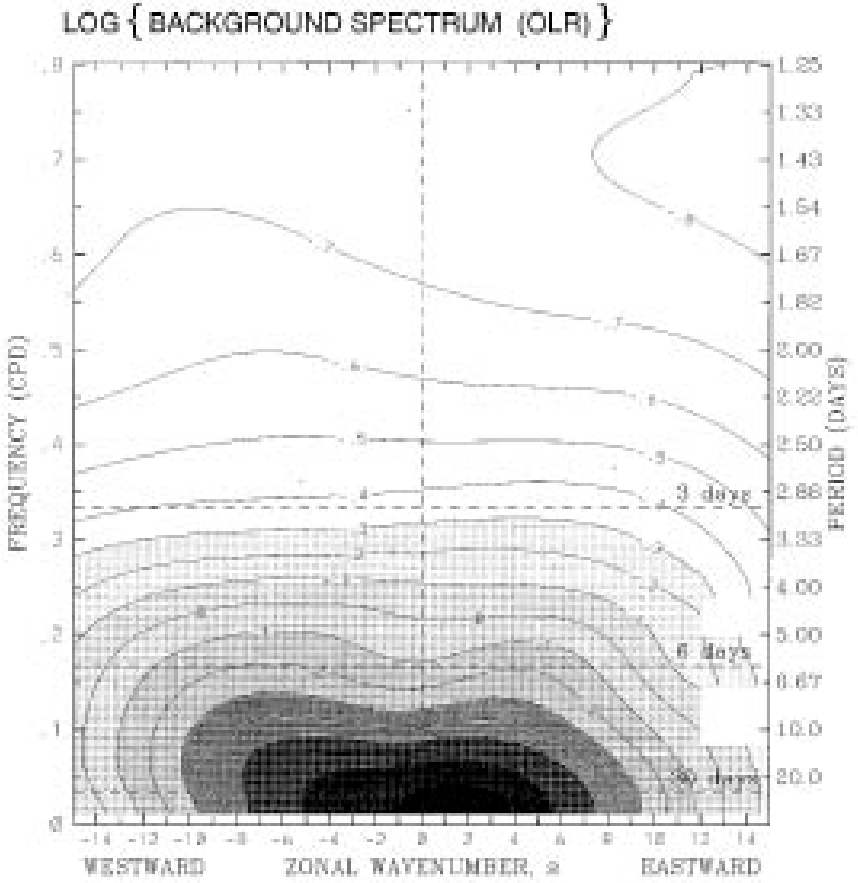

FIG. 2. Zonal wavenumber-frequency spectrum of the base-10 logarithm of the "background" power calculated by averaging the individual power spectra of Figs. 1a and 1b, and smoothing many times with a 1-2-1 filter in both wavenumber and frequency. The contour interval and shading are the same as in Fig. 1.

Sym & anti-sym spectra divided by background. Equivalent depths ~10-50 m means phase speeds 10-25 m/s. Dry waves would have 50 m/s.

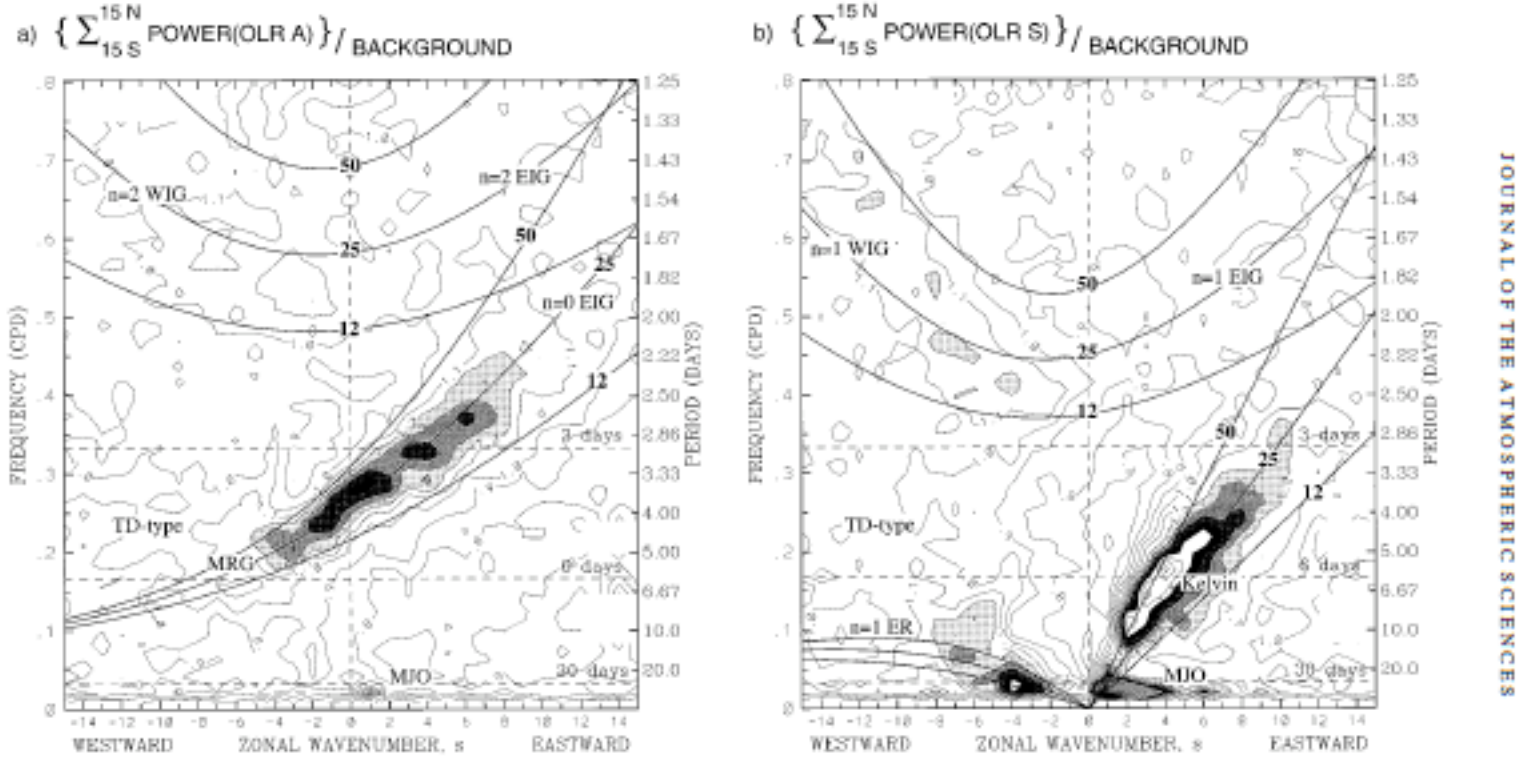

FIG. 3. (a) The antisymmetric OLR power of Fig. 1a divided by the background power of Fig. 2. Contour interval is 0.1, and shading begins at a value of 1.1 for which the spectral signatures are statistically significantly above the background at the 95% level (based on 500 dof). Superimposed are the dispersion curves of the even meridional mode-numbered equatorial waves for the three equivalent depths of h = 12, 25, and 50 m. (b) Same as in panel a except for the symmetric component of OLR of Fig. 1b and the corresponding odd meridional mode-numbered equatorial waves. Frequency spectral bandwidth is 1/96 cpd.

JOURNAL OF THE ATMOSPHERIC SCIENCES

Spectral bands used to reconstruct dynamical signals associated with each wave type

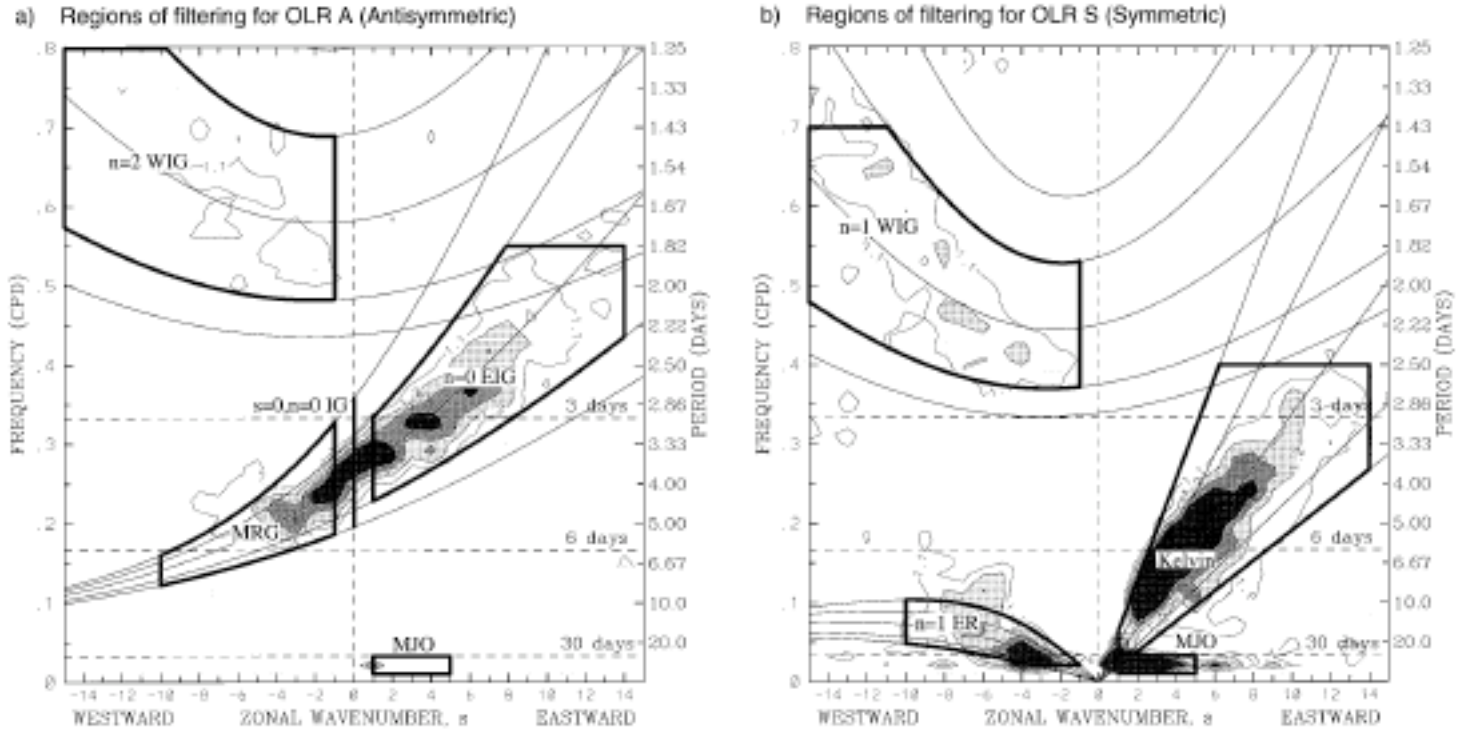

FIG. 6. As in Fig. 3 excluding contours less than 1.1 and greater than 1.4. Thick boxes indicate the regions of the wavenumber-frequency domain used for filtering of the OLR dataset to retrieve the longitude-time information of the convectively coupled tropical waves for the (a) antisymmetric component and (b) symmetric component of the OLR. The thin lines are the various equatorial wave dispersion curves for the five different equivalent depths of h = 8, 12, 25, 50, and 90 m.

Composite Kelvin wave: OLR, 200 hPa geopotential and wind obtained by regression against time series of Kelvin-filtered OLR at base point 0N, 90E

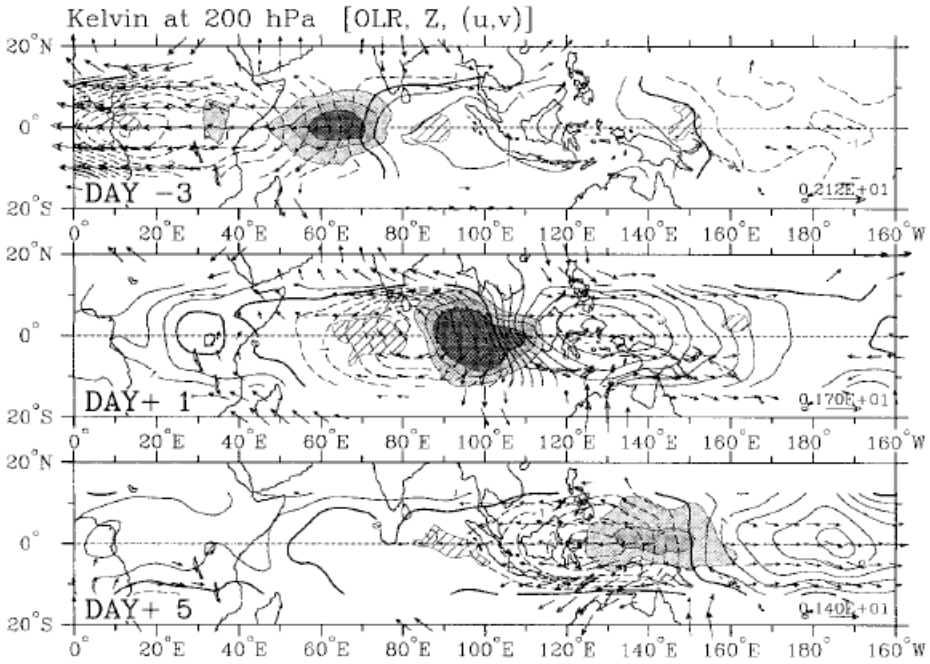

FIG. 5. Maps of OLR (hatching/shading), 200-hPa geopotential height (contours), and 200-hPa wind (vectors) anomalies associated with the OLR variation of the convectively coupled Kelvin wave at the base point 0°, 90°E, for day −3, day +1, and day +5. Hatching denotes OLR anomalies greater than 5 W m^{-2}, and the three levels of shading denote OLR anomalies less than −5, −10, and −15 W m^{-2}, respectively. Contours are shown only for latitudes equatorward of 15°, and the contour interval is 0.5 m, with negative contours dashed. Wind vectors are locally statistically significant at the 95% level, with the largest vectors as shown in the bottom-right corner.

Theoretical Kelvin height & flow field from shallow water eqns

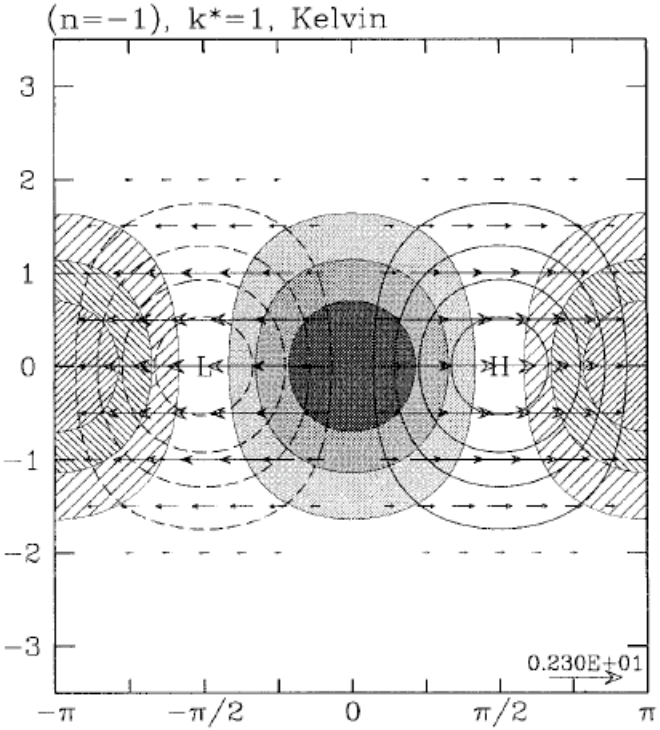

FIG. 6. The theoretical equatorially trapped Kelvin wave solution to the linear shallow water equations on an equatorial β plane (Matsuno 1966) for a nondimensional zonal wavenumber 1. Hatching is for convergence and shading for divergence, with a 0.6 unit interval between successive levels of hatching or shading, and with the zero divergence contour omitted. Unshaded contours are for geopotential, with a contour interval of 0.5 units. Negative contours are dashed and the zero contour is omitted. The largest wind vector is 2.3 units, as marked. The dimensional scales are as in Matsuno (1966).

Kelvin vertical velocity, temperature, vertical & zonal wind wrt longitude & height

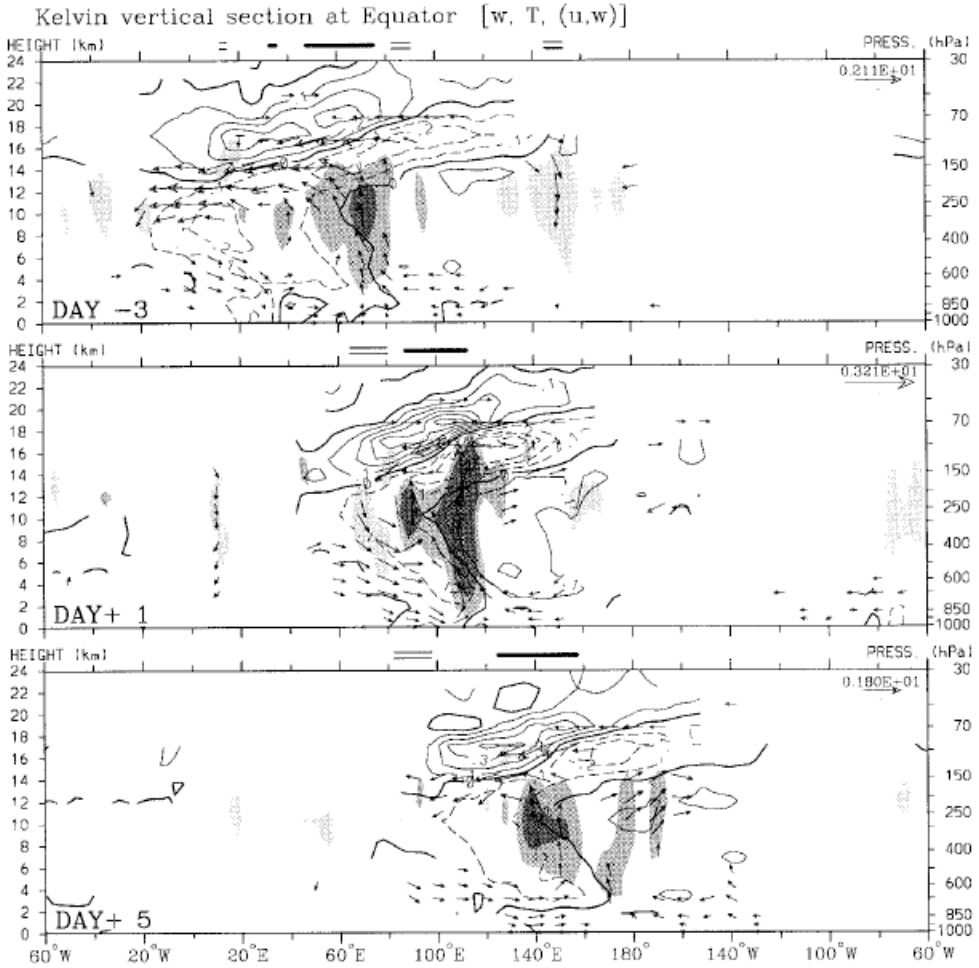

FIG. 7. Longitude–height cross sections along the equator of the vertical velocity (shading), temperature (contours), and zonal-vertical wind (vectors) anomalies associated with the OLR variation of the convectively coupled Kelvin wave at the base point 0°, 90°E, for day −3, day +1, and day +5. Lightest shading shows downward velocity <-0.1 cm s^{-1}, medium shading for upward velocity >0.1 cm s^{-1}, and darkest shading for upward velocity >0.2 cm s^{-1}. Contour interval for temperature is 0.1 K, with negative contours dashed. Vector vertical wind component is multiplied by a factor of 500, and the largest labeled vectors (top-right corner) are in units of meters per second. Single and double bars at the top of each plot show the positions of the OLR anomalies <-5 W m^{-2} and >5 W m^{-2}, respectively. Wind vectors are locally statistically significant at the 99% level, and the contours are only shown within two levels vertically or 15° horizontally of points that are locally significant at the 99% level.

Composite n=1 equatorial Rossby wave, OLR and 850 hPa stream fn & wind

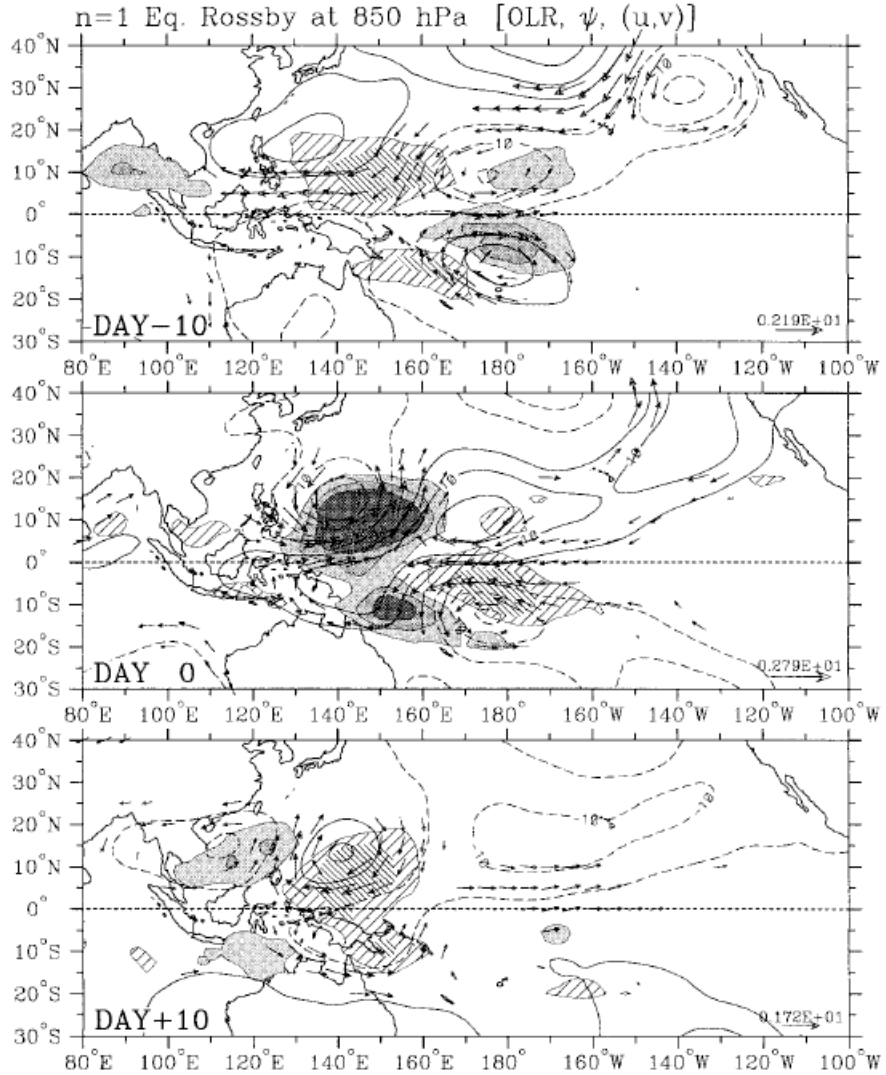

FIG 9. As in Fig. 5 except for 850-hPa horizontal streamfunction (contours), and wind (vectors) anomalies associated with the convectively coupled $n = 1$ equatorial Rossby wave at the base point 10°S, 150°E, at day −10, day 0, and day +10. The two levels of hatching denote OLR anomalies greater than 5 and 10 W m^{-2}, and the three levels of shading denote OLR anomalies less than −5, −10, and −15 W m^{-2}, respectively. Contour interval is 5×10^5 m^2 s^{-1}, with negative contours dashed and the zero contour omitted.

Theoretical n=1 Rossby

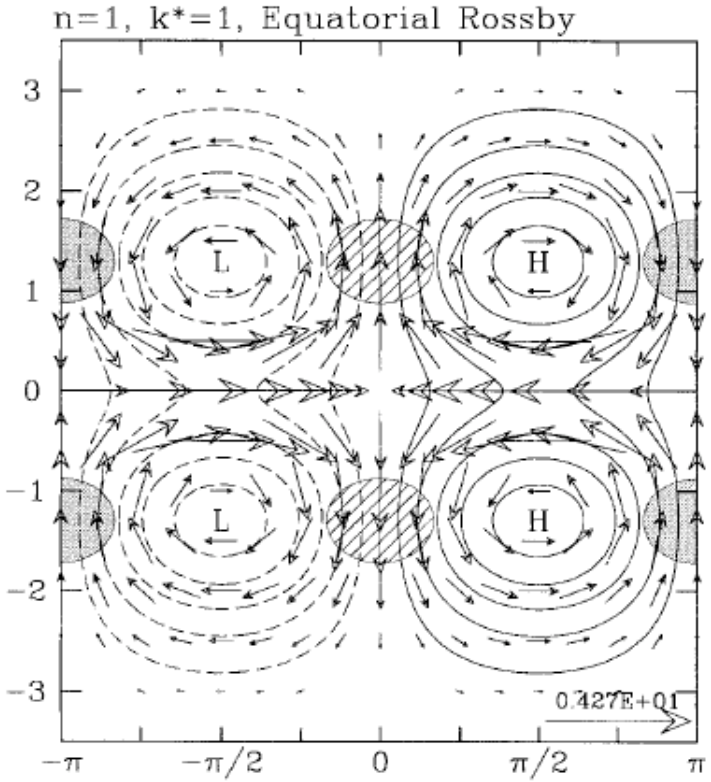

FIG. 10. As in Fig. 6 except for the $n = 1$ ER wave.

MRG OLR, stream fn, wind at 3 levels

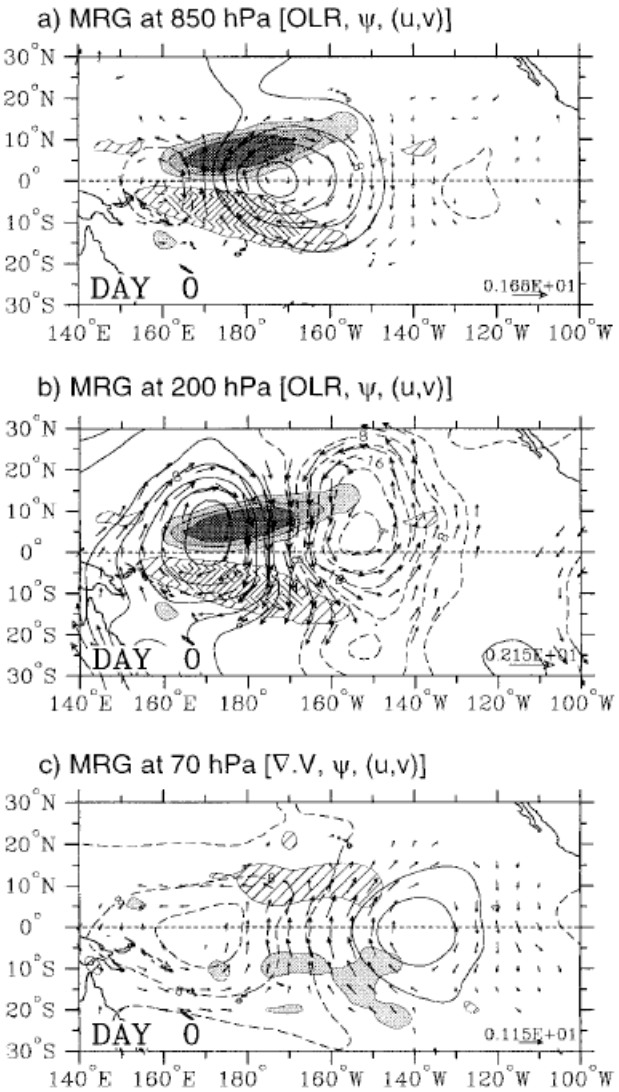

Theoretical MRG

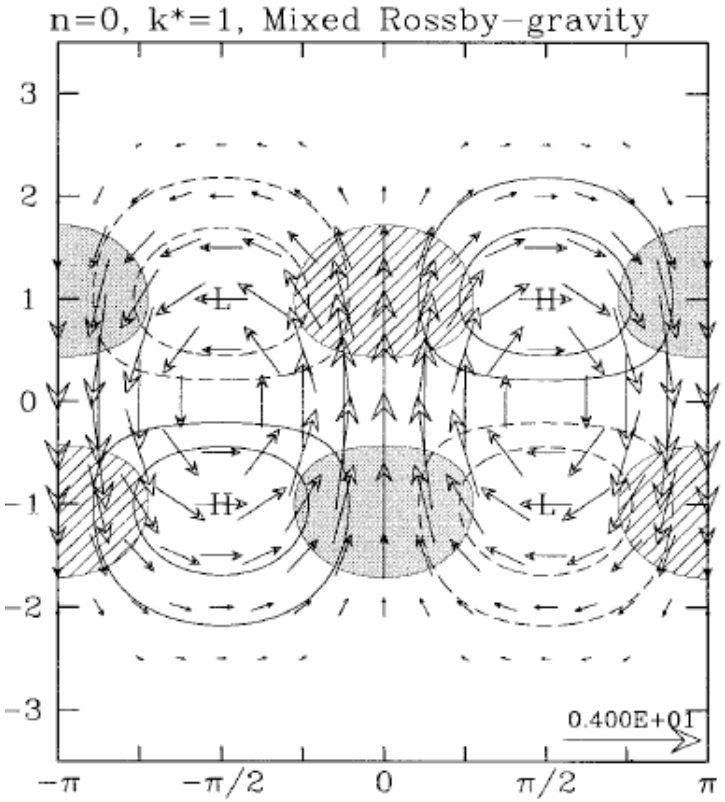

FIG. 14. As in Fig. 6 except for the MRG wave.

Easterly/TD-type waves are a mainly northern summer phenomenon: wavenumber-frequency OLR spectrum for June-August (Kiladis et al. 2006)

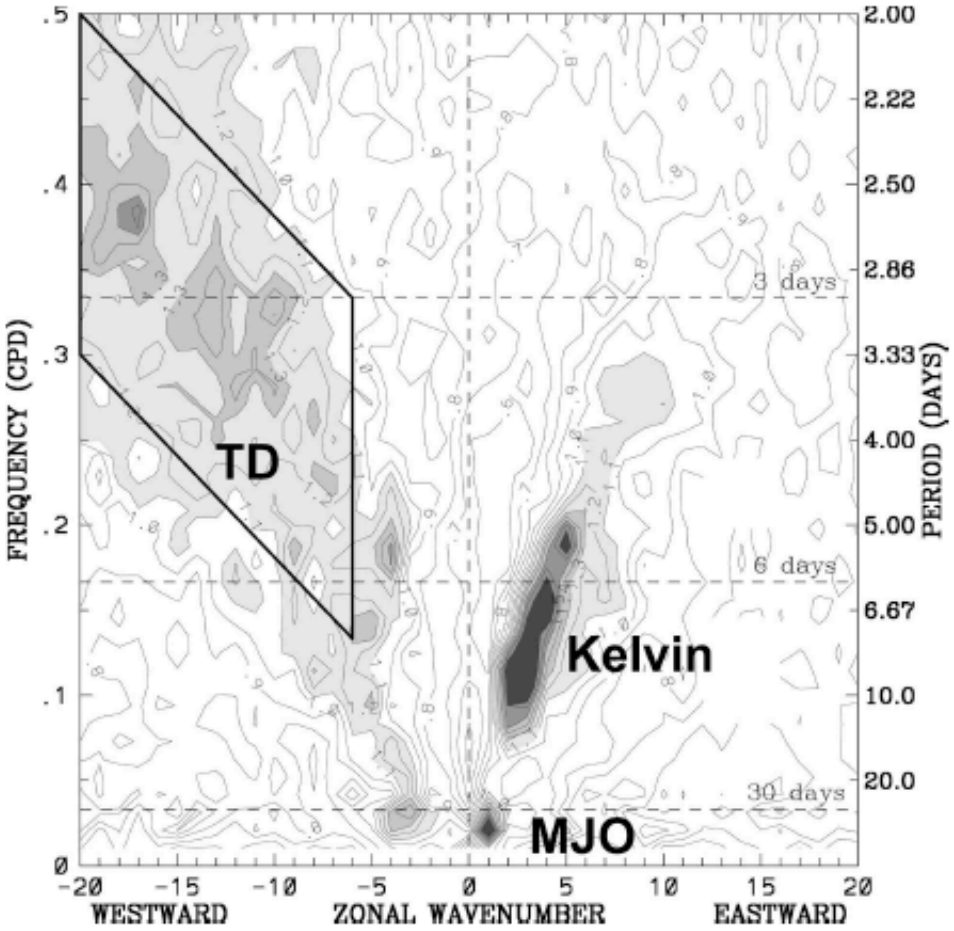

FIG. 1. Wavenumber–frequency power spectrum of the symmetric component of OLR for June–August 1979–2003, averaged from 15°N to 15°S, plotted as the ratio of the raw OLR spectrum against a smooth red noise background (see WK99 for details). Contour interval is 0.1. Shading begins at 1.1, where the signal is significant are greater than approximately the 95% level. Heavy solid box represents the region of TD wave filtering, and the spectral peaks of the MJO and Kelvin waves are also identified.

Longitude-height composites of western Pacific easterly waves (Reed and Recker 1971)

Meridional wind

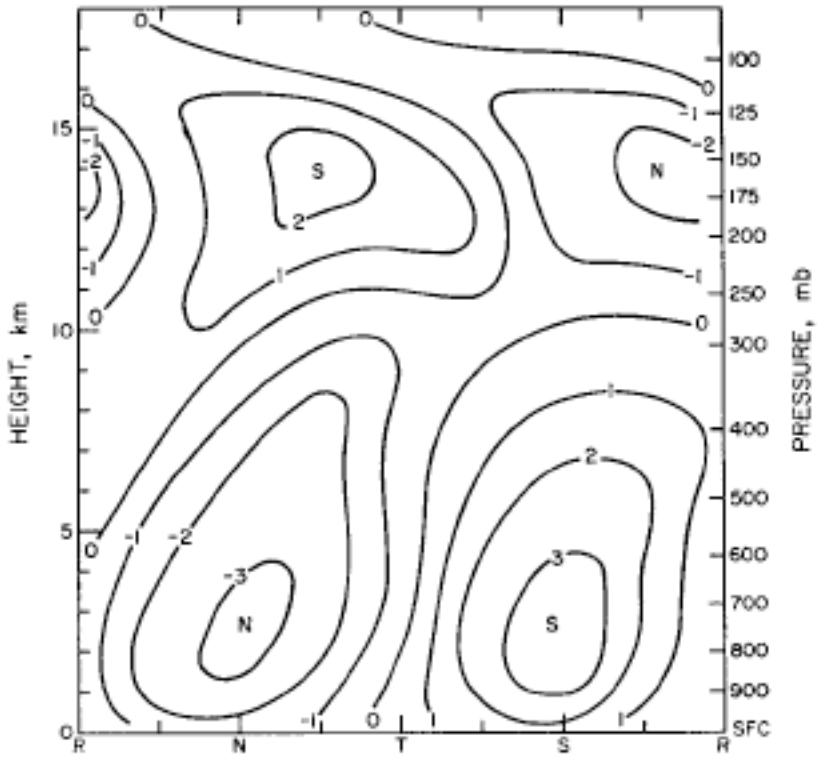

FIG. 4. Composite diagram of meridional wind speed (m sec^{-1}) for KEP. The letters R, N, T and S refer to the ridge, north wind, trough and south wind regions, respectively, of the wave as defined by its structure in the lower troposphere.

Time mean zonal Wind for 3 stations

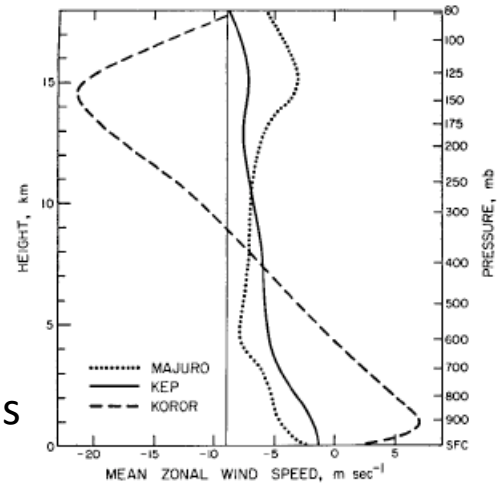

FIG. 3. Mean zonal wind speed for the period July–September 1967. The profile labeled KEP is the mean for Kwajalein, Eniwetok and Ponape. The thin vertical line denotes the average wave speed (−9 m sec^{-1}) observed during the period of study.

Relative humidity

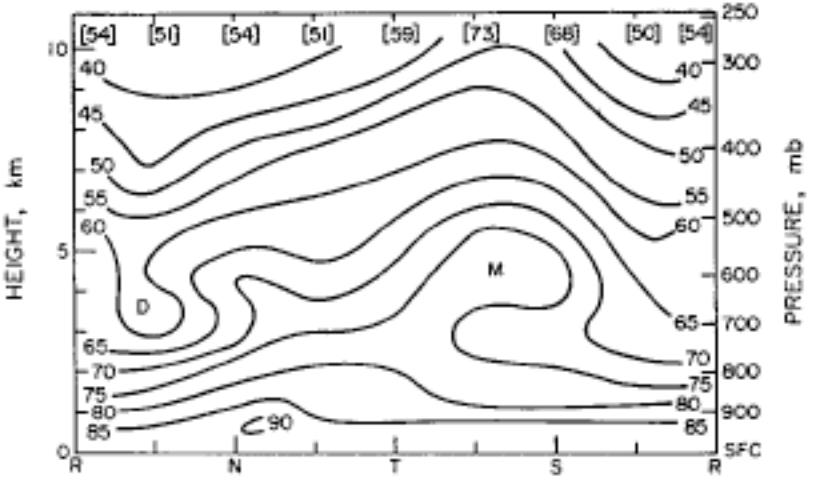

FIG. 6. Composite diagram of relative humidity for KEP. Values in brackets at the top are for saturation with respect to ice. Refer to Fig. 4 for further explanation.

Horizontal divergence and omega

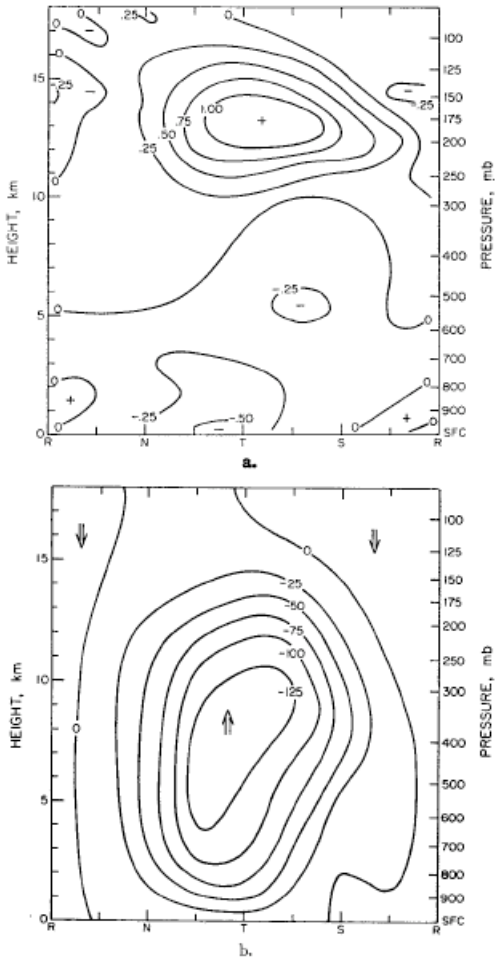

FIG. 8. Composite of horizontal velocity divergence (10^{-5} sec^{-1}) for KEP, a., and corresponding vertical p velocity (10^{-5} mb sec^{-1}), b. (Analyzed values give approximate displacement in millbars per day.) See Fig. 4 for further explanation.

Relative vorticity

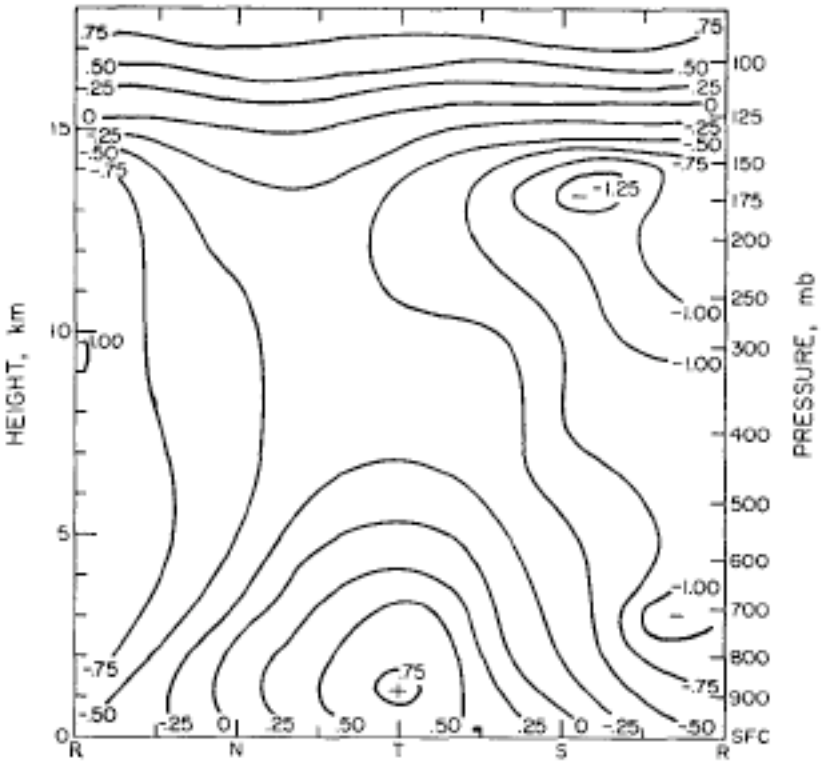

FIG. 9. Composite diagram of vertical component of relative vorticity (10^{-5} sec^{-1}) for KEP. See Fig. 4 for further explanation.

Temperature perturbations very small compared to heating – heating is balanced by vertical advection of potential temperature (just as in climatology)

Temperature perturbations

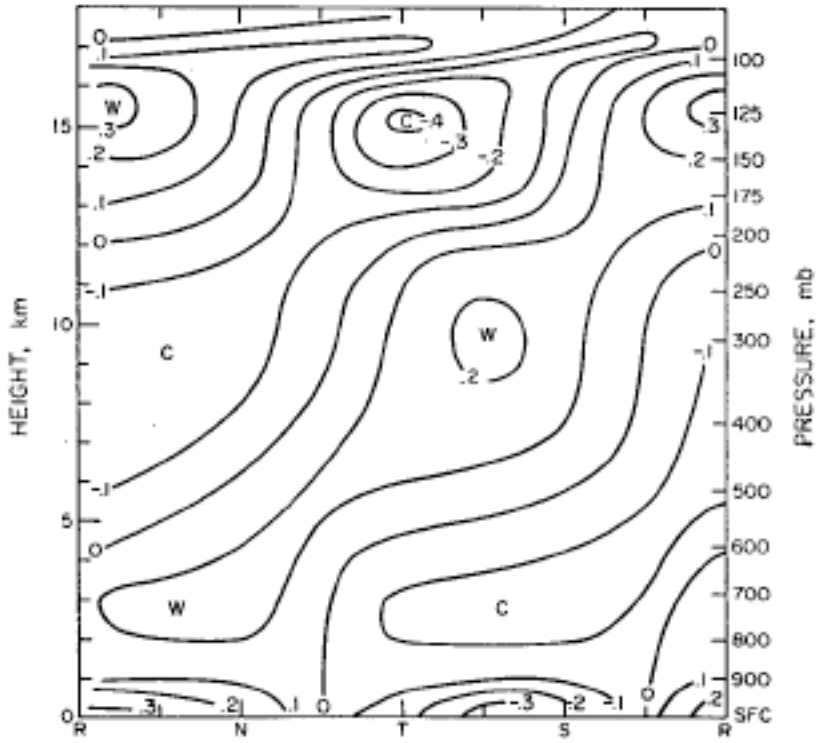

FIG. 5. Composite diagram of temperature deviations (°C) at various levels from their respective mean values at KEP. Refer to Fig. 4 for further explanation.

Diabatic heating Q1

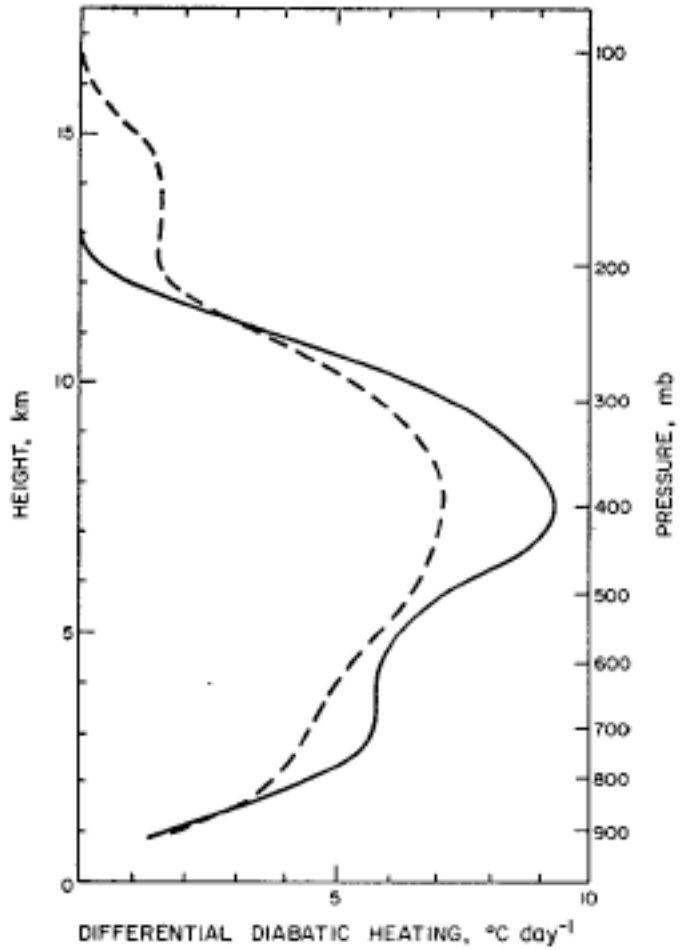

FIG. 14. Diabatic heating difference between trough and ridge areas: solid line, model with effects of convection included explicitly; dashed line, simple model.

Moisture budget: precipitation variations mostly balanced by moisture convergence (also as in climatology)

TABLE 1. Computed moisture budget (cm day^{-1}). Category 4 is centered on the trough axis, category 8 on the ridge.

	Category								
	1	2	3	4	5	6	7	8	Mean
Storage	−0.25	−0.36	−0.06	−0.02	0.01	0.28	0.30	0.11	0
Advection	0.09	0.18	−0.04	−0.18	−0.35	−0.30	−0.30	−0.14	−0.13
Convergence	0.17	0.76	1.52	1.38	0.83	0.17	0.07	−0.10	0.60
Sum $= P - E$	0.01	0.58	1.42	1.18	0.49	0.15	0.07	−0.13	0.47
Evaporation	0.25	0.27	0.32	0.35	0.39	0.32	0.26	0.26	0.30
Precipitation	0.26	0.85	1.74	1.53	0.88	0.47	0.33	0.13	0.77

Some individual events, from KWAJEX field experiment, Kwajalein, Republic of Marshall Islands, Jul-Sep 1999

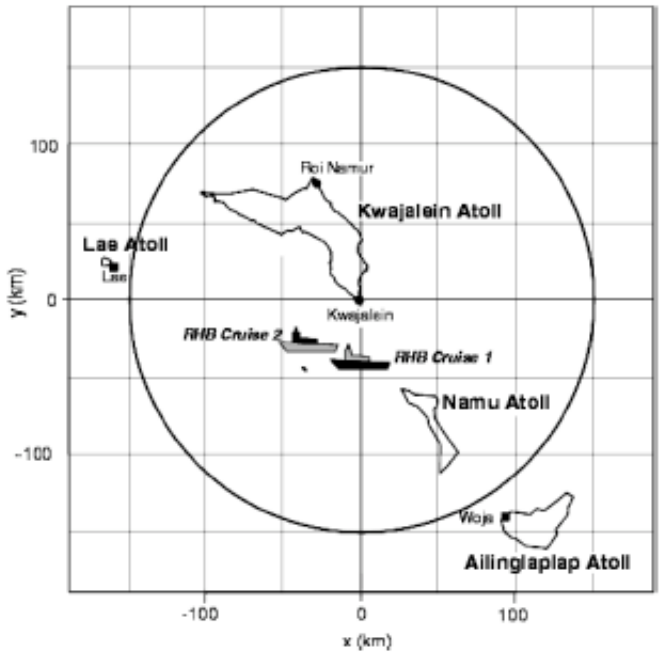

FIG. 1. Map showing the KWAJEX study area, including rawinsonde sites on the R/V *Ronald H. Brown* (RHB) and at Kwajalein, Lae, Roi-Namur, and Woja on the edges of largely submerged coral atolls. A 150-km-range circle around the Kwajalein ground-validation radar encompasses the region over which our radar-based precipitation estimates are taken. The latitude and longitude of Kwajalein are 8.72°N, 167.73°E.

Slides on observed convectively coupled waves here.

Tropical wave theory, 9

Instead of free waves, we can study the **steady, forced-dissipative problem** in the dry system, with convective heating treated as external (Webster 1972; Gill 1980)

$$-\beta y v = -\frac{\partial p}{\partial x} - \epsilon u$$

$$\beta y u = -\frac{\partial p}{\partial x} - \epsilon v$$

$$\frac{\partial u}{\partial x} + \frac{\partial v}{\partial y} = Q - \epsilon_T p$$

Q can have any spatial structure, but we consider a zonally and meridionally localized forcing centered on the equator. For generaity we have allowed momentum and thermal damping coefficients ϵ and ϵ_T to be different (Gill did not).

Tropical wave theory, 10

(a) Vertical velocity (contour) & low-level horizontal velocity; (b) horizontal velocity and pressure; (c) circulation in longitude-height plane.

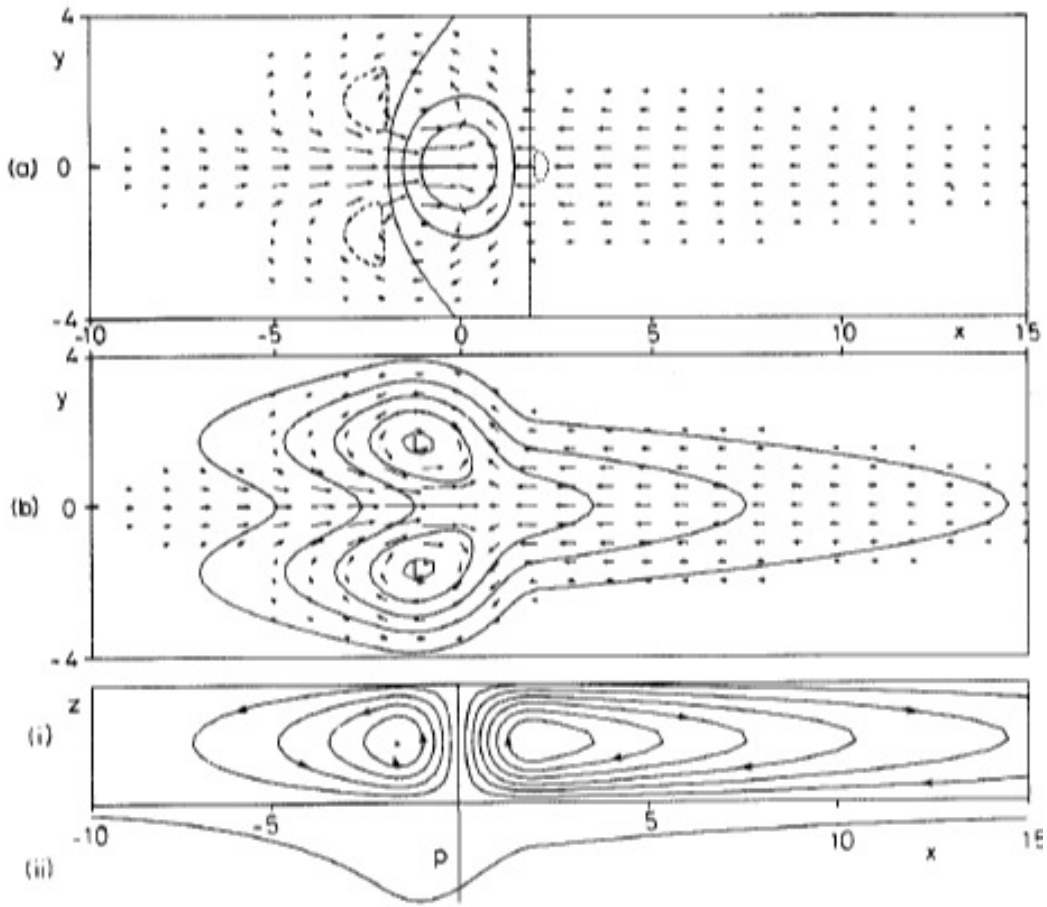

Gill (1980, *Q. J. Royal Met. Soc.*).

Interaction of convection with large-scale waves -1

We are particularly interested in the way in which **interactive convection** — Q_c a function of the resolved prognostic variables — changes the dynamics.

The simplest case to consider is a gravity wave in two dimensions. We imagine that there is no vertical propagation — not really true, but adequate for qualitative discussion. (Vertical propagation will cause "leakage" of wave energy to the stratosphere.)

Assume we have a boundary layer whose thermodynamic properties are fixed, and a troposphere with stable stratification (to dry displacements), $N > 0$. Ascent cools the troposphere, increasing CAPE; descent warms, decreasing CAPE.

Interaction of convection with large-scale waves -2

Now assume that the wave is acting against a background state in which precipitation is constantly occurring (in a statistical sense); could be RCE (but doesn't have to be).

If we assume the convection is in instantaneous statistical equilibrium with the large-scale dynamical changes induced by the wave — e.g. moist **convective adjustment — convection will act to oppose the changes in CAPE**. It will heat the troposphere when there is ascent (and cool the PBL by downdrafts), cool the troposphere when there is descent.

Interaction of convection with large-scale waves -2.5

If we assume that the convective changes do not exceed the changes due to large-scale ascent/descent — which makes sense if they are responses to it — then the effect, if it is instantaneous, is to **reduce the effective stratification** (e.g., Emanuel, Neelin and Bretherton, 1994, QJRMS). **This is one theory for the observed fact that convectively coupled waves have slower phase speeds than their dry counterparts** with first baroclinic mode structure.

Another plausible argument is that real convectively coupled waves are not pure first baroclinic mode, but have a second baroclinic mode component because of stratiform heating. The second mode has smaller phase speed even in dry theory, and may control the phase speed of the combined mode (see papers by Mapes, Kuang, Majda and colleagues).

Interaction of convection with large-scale waves -3

Simulated convectively coupled gravity wave (Sobel and Bretherton 2003, *Tellus*). y-axis is $\sigma = p/p_0$. Phase speed 30 m/s, vs. dry 50.

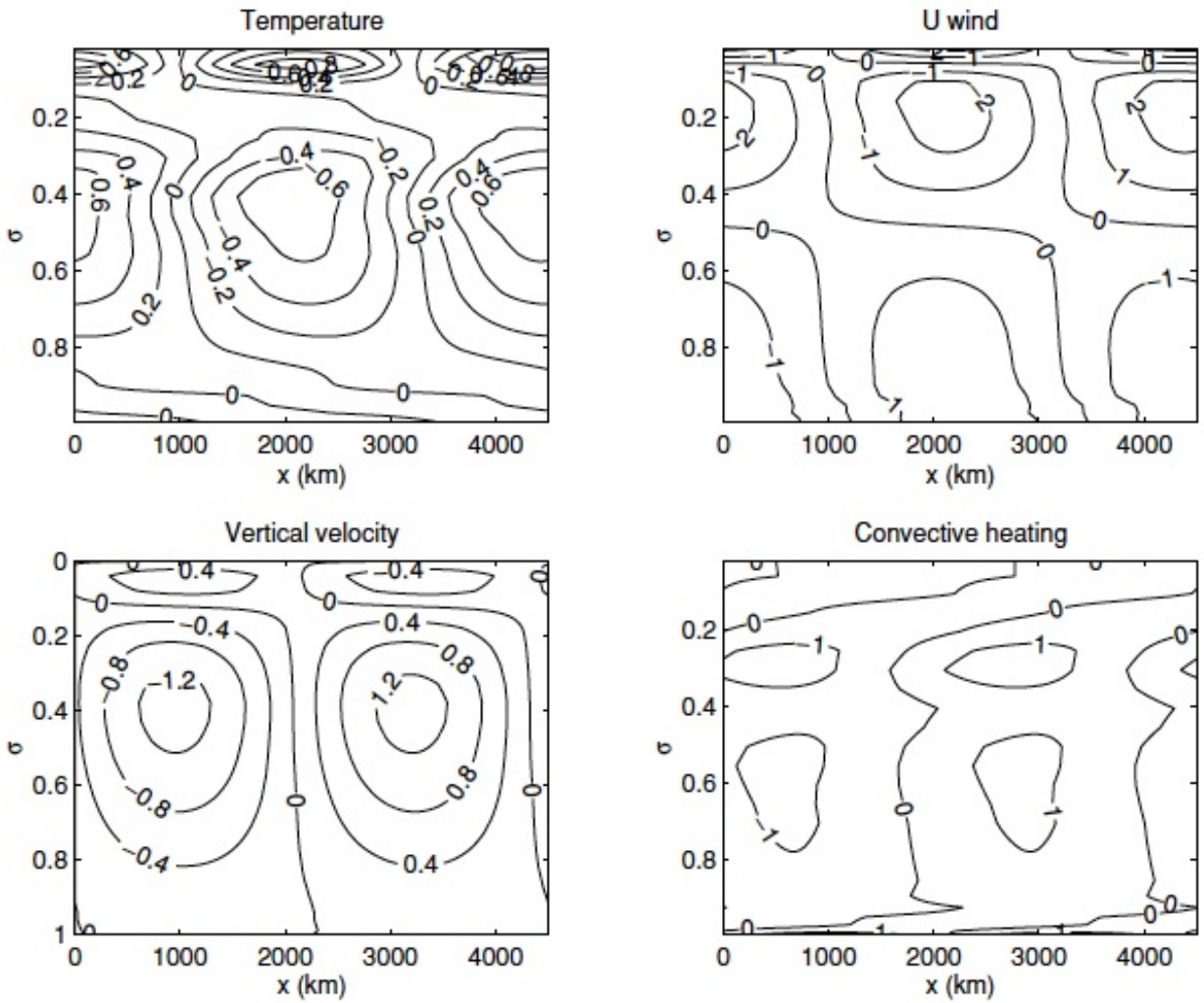

Interaction of convection with large-scale waves -4

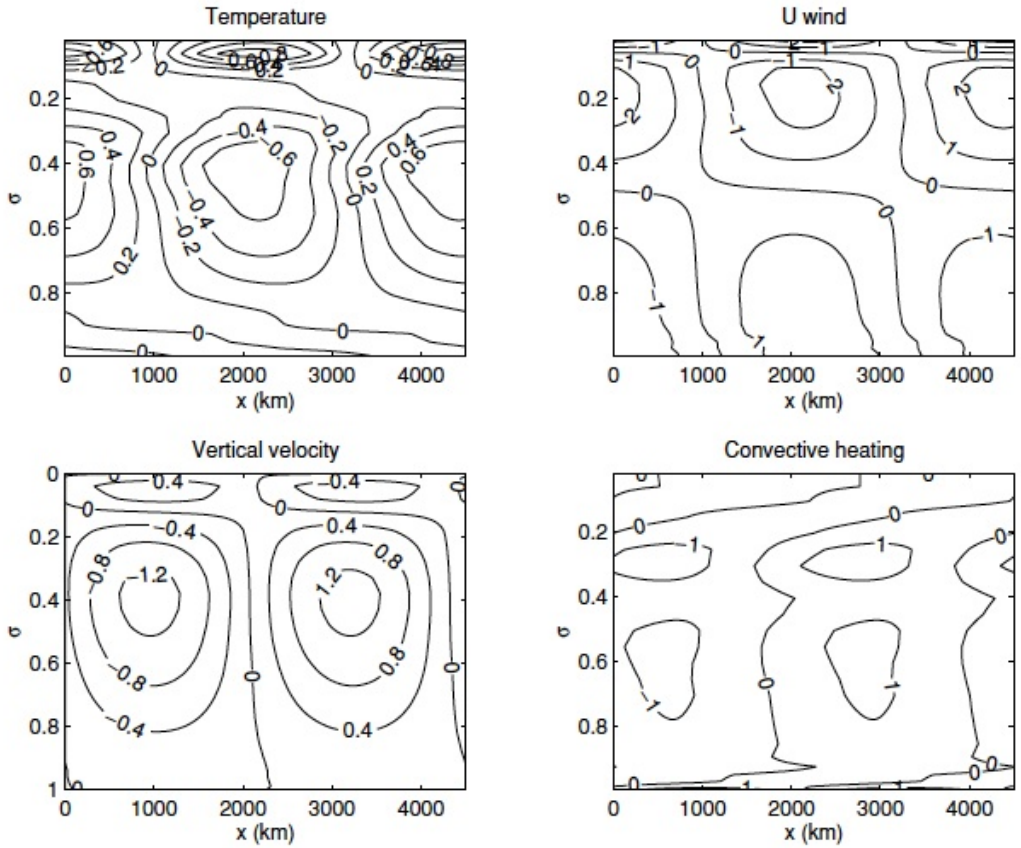

Actually, the convection takes a finite time to respond to the convection. As a result the convective heating has some overlap with the cold temperature anomaly, resulting in **moist convective damping**:

Interaction of convection with large-scale waves -4

If we have

$$\frac{\partial T}{\partial t} + wN^2 = Q$$

multiply by T and average over wave phase

$$\frac{1}{2}\frac{\partial}{\partial t}\overline{T^2} + N^2\overline{wT} = \overline{QT}$$

to first order w and T are in quadrature (exactly so for $Q = 0$) but shifting Q to be partly out of phase with T will make $\overline{QT} < 0$, thus damping temperature variance.

Interaction of convection with large-scale waves -5

At the same time, if we have something which makes Q be in phase with T, that will lead to disturbance growth. An example could be surface fluxes.

Surface fluxes create CAPE, by adding buoyancy (increasing T and q) to boundary layer air. If convection responds instantaneously (or at least quickly), positive Q anomalies will follow.

This led to the "wind-evaporation feedback" (Neelin et al. 1987) or "wind-induced surface heat exchange" (WISHE; Emanuel 1987) theory of the Madden-Julian oscillation.

Interaction of convection with large-scale waves -6

Emanuel (87) and Neelin et al. (87) proposed that the MJO is a Kelvin wave driven by wind-induced surface fluxes ("WISHE")

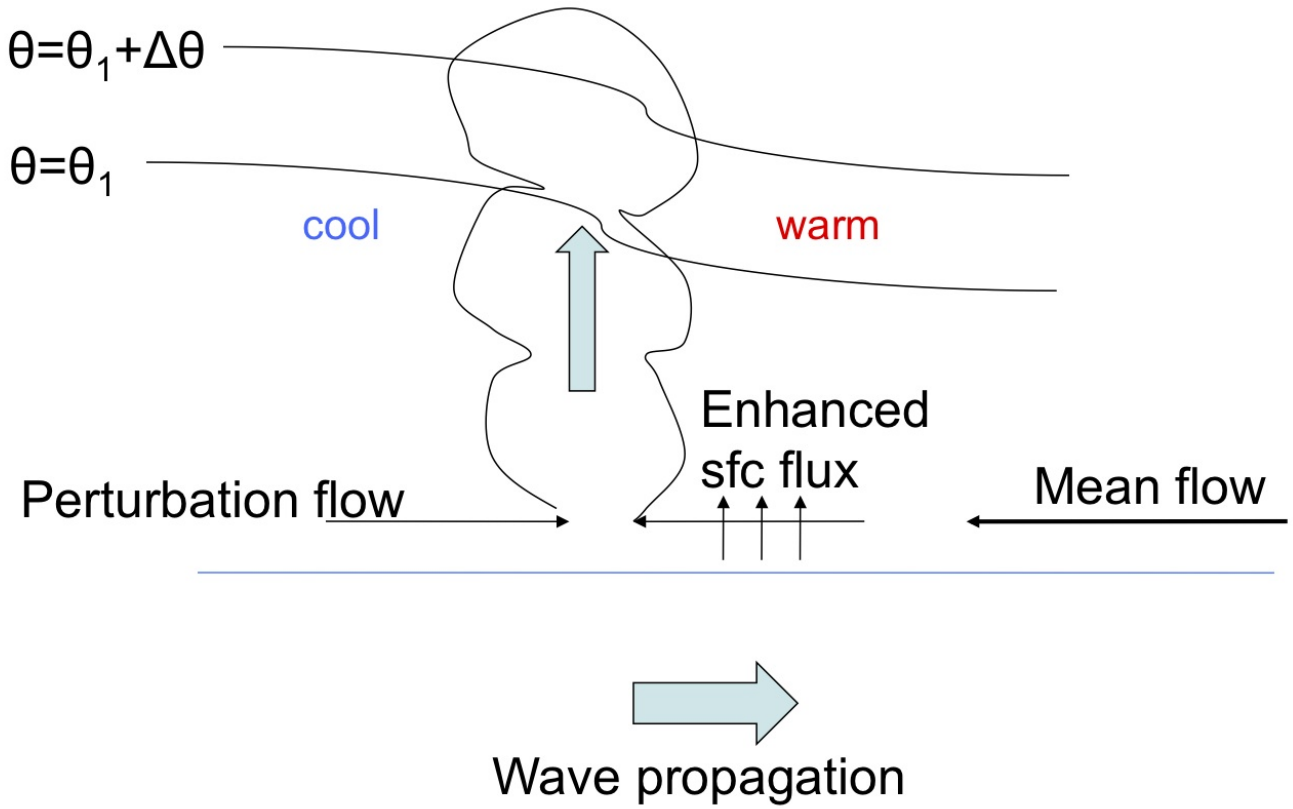

Interaction of convection with large-scale waves -7

These ideas — and really almost all early tropical dynamics theories — treat moisture as diagnostic. Relative humidity is typically assumed constant, or predicted in a way that slaves it tightly to the large-scale fields. Convection thus becomes a function either of just temperature (moist convective adjustment) or large-scale convergence. The presence of moisture just modifies existing dry wave modes.

However, if we have truly prognostic moisture, then there should be a new mode of behavior, in a linear model. We call this a **moisture mode**. How it behaves will depend on physics.

An example from Sobel and Bretherton (2003). (See also many papers by Dave Raymond, Zeljka Fuchs and associates.)

Interaction of convection with large-scale waves -8

This mode is a blob of moisture that moves with the environmental flow (here 5 m/s) and decays slowly. **No radiative feedback** in this simulation.

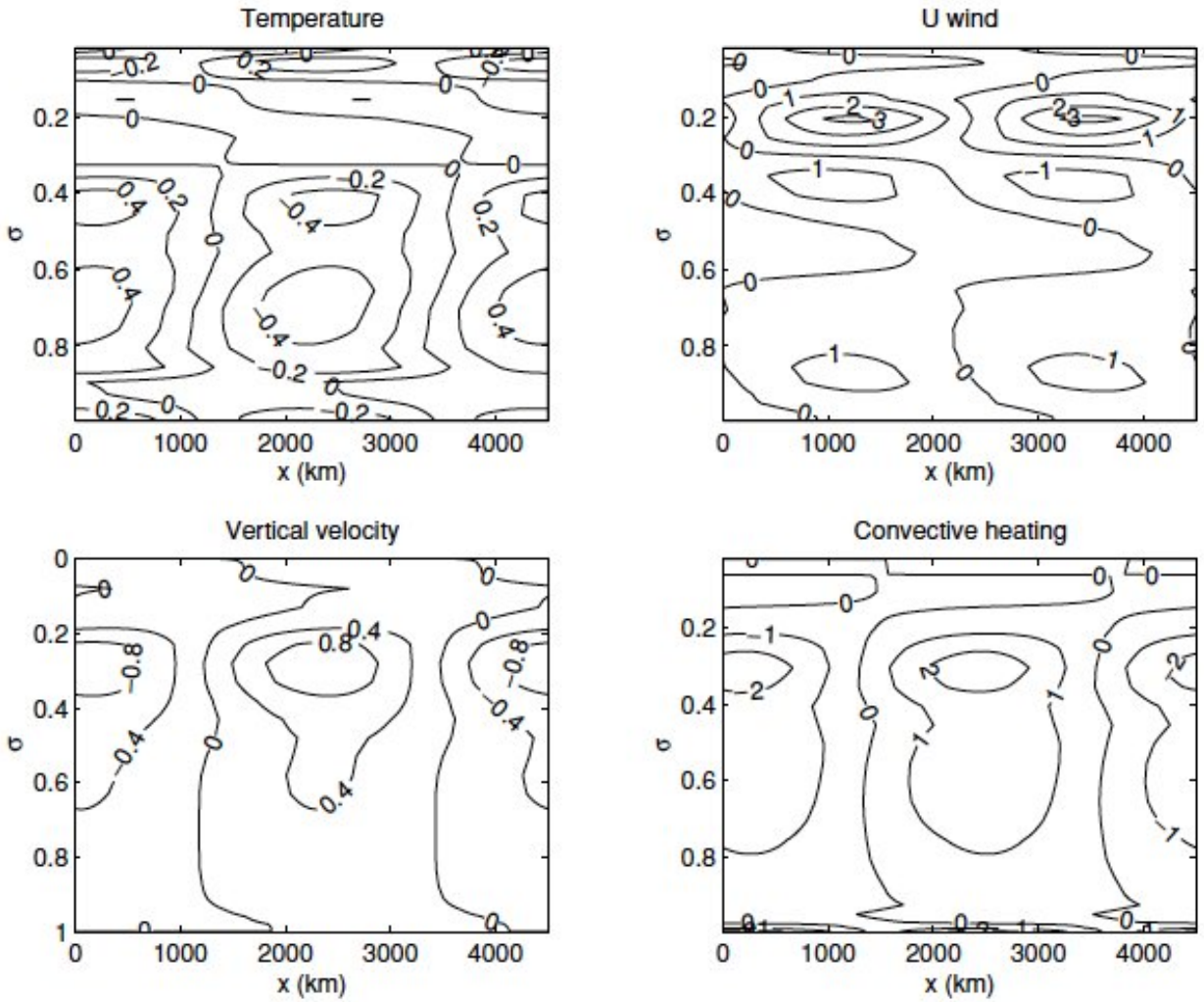

Interaction of convection with large-scale waves -9

Moisture and precpitation in the convectively coupled gravity wave.

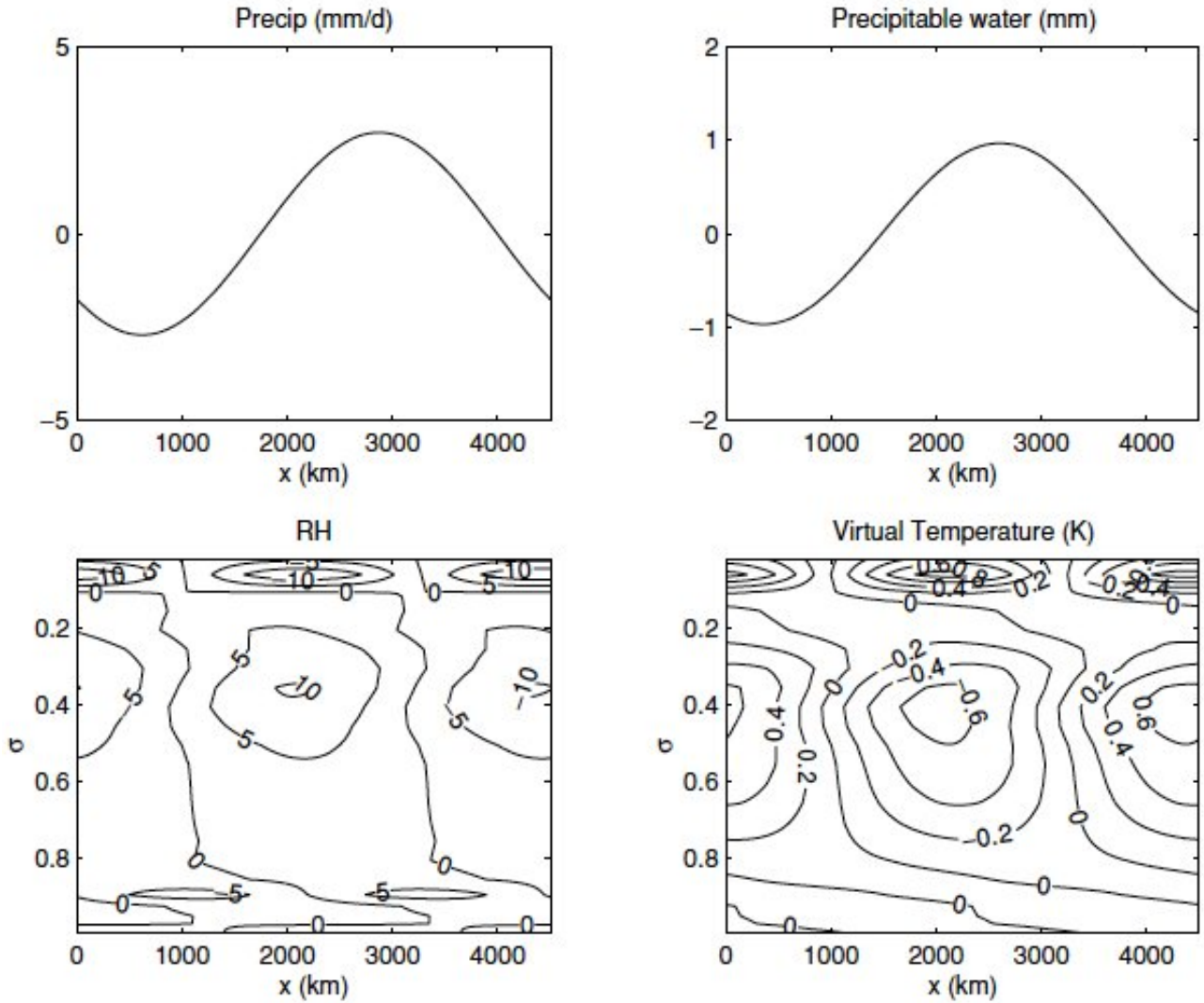

Interaction of convection with large-scale waves -10

Moisture and precipitation in the moisture wave.

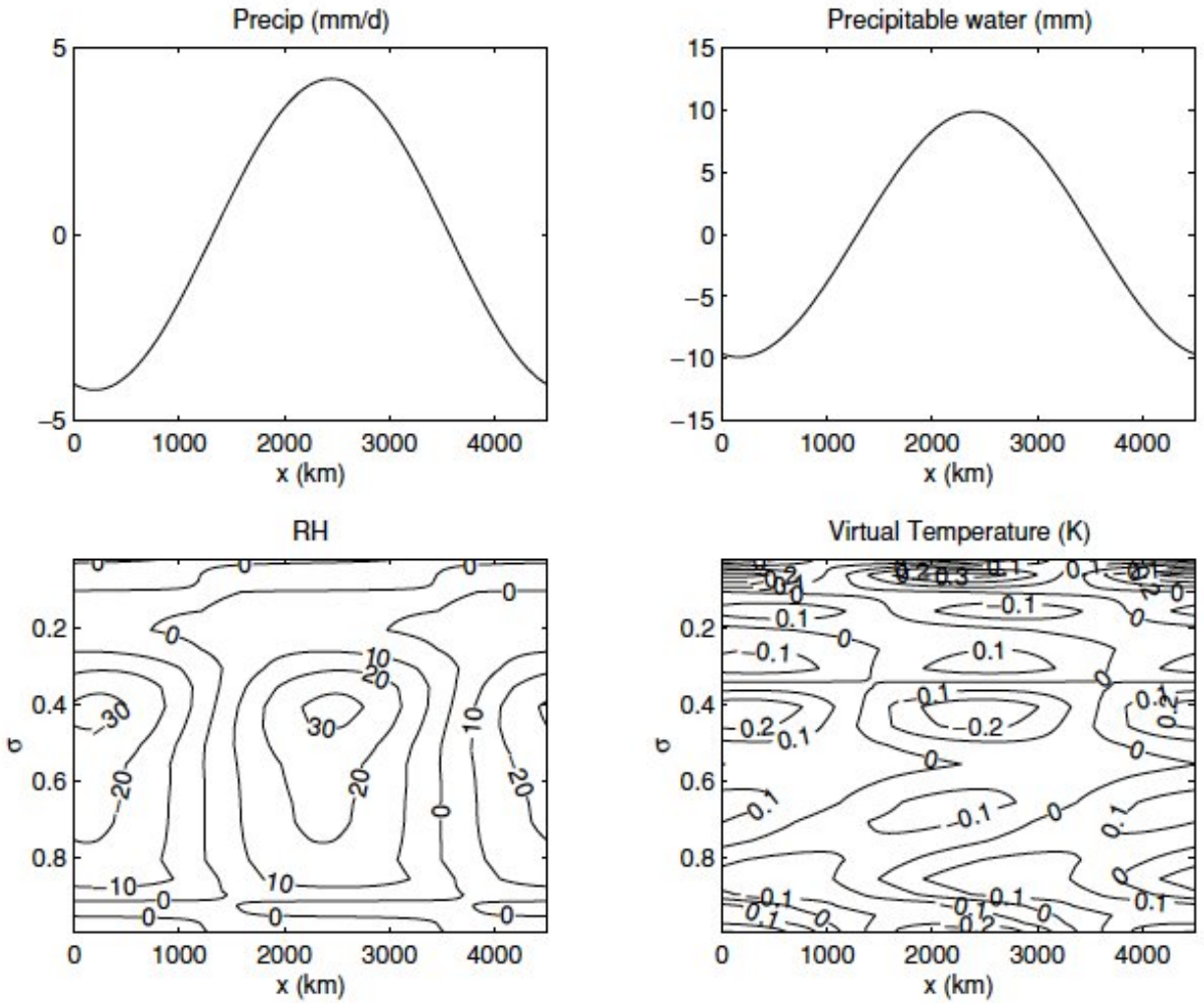

Interaction of convection with large-scale waves -11

A current theory of tropical cyclogenesis, known as "marsupial" (Dunkerton et al. 2009, *Atmos. Chem. Phys*) holds that the incipient cyclone is essentially a blob of moist air that needs to be protected by closed streamlines against dry air advection.

Montgomery web page

Interaction of convection with large-scale waves -12

Montgomery et al. (2010, *Atmos. Chem. Phys.* **10**, 9879-

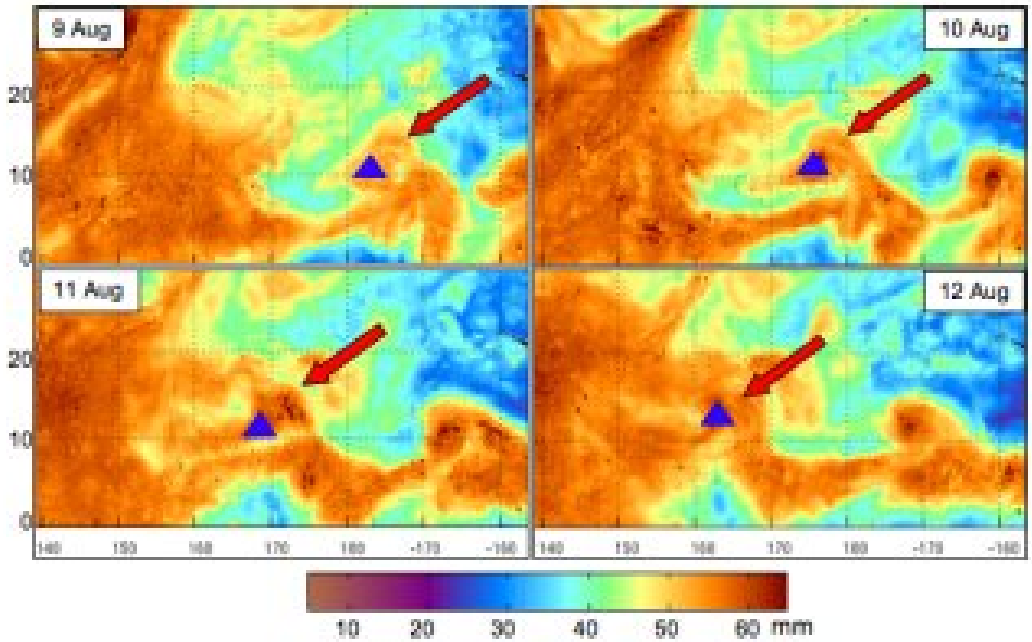

Fig. 6. Four-day time series of CIMMS Morphed TPW valid at 12:00 Z each day. Red arrows point towards the cat's eye region of the easterly wave (i.e., the wave pouch), which is hypothesized by DMW09 to be an area of increased moisture in the low to mid-troposphere and which helps protect the proto-vortex from lateral intrusions of dry air. The blue triangles indicate the position of the sweet spot as diagnosed in the GFS FNL at the 925 hPa level.

Interaction of convection with large-scale waves -13

Montgomery et al. (2010, *Atmos. Chem. Phys.* **10**, 9879-

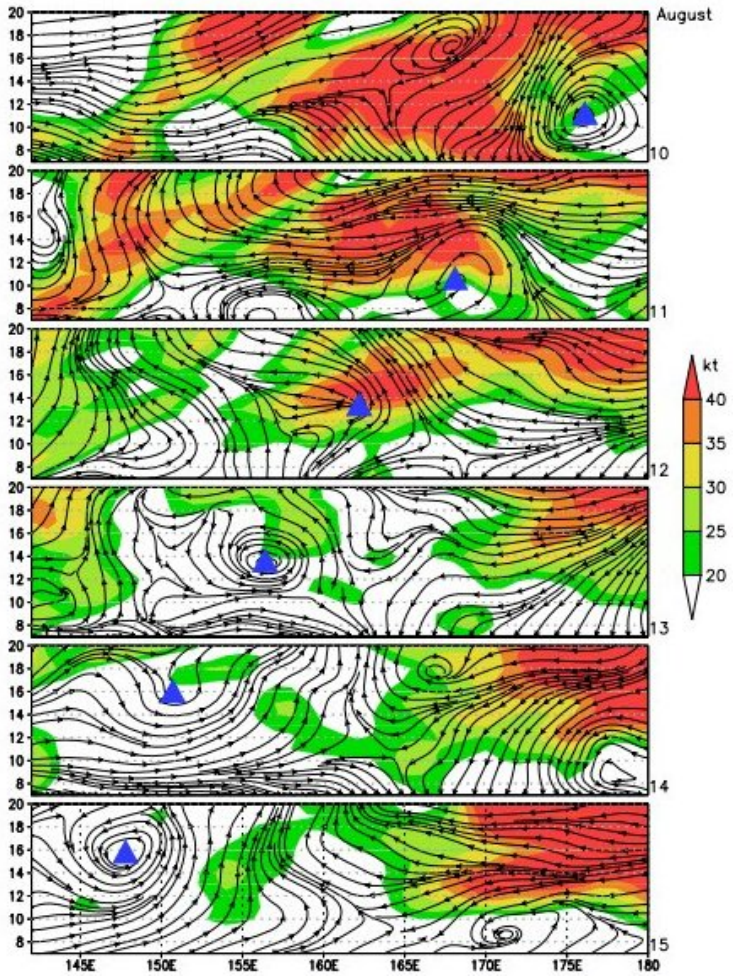

Vertical wind shear (850-200 hPa), 925 hPa co-moving streamlines.

Self-aggregation - 1

When non-rotating radiative-convective equilibrium simulations are run in **cloud-resolving models** (resolution $\sim 1km$, can simulate large cloud updrafts but not all turbulence), on a small domain, convection is "popcorn" in appearance — distributed randomly throughout the domain.

But if the domain is large enough, convection **self-aggregates** to a single spot, which can last indefinitely. The rest of the domain becomes very dry.

Bretherton et al. (2005) precipitation (P), water vapor path (WVP), total surface heat flux, outgoing longwave radiation (OLR), day 10 of simulation.

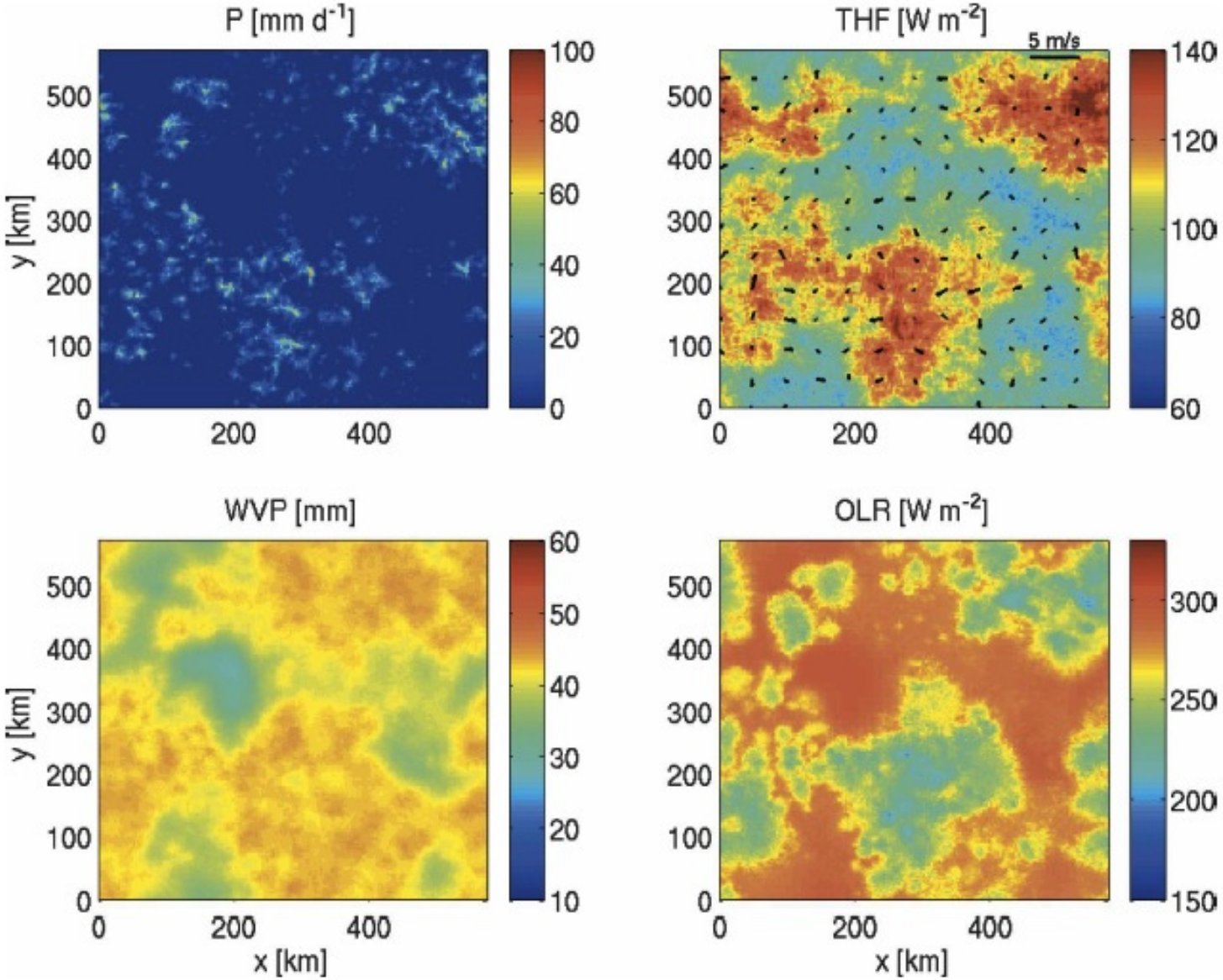

Bretherton et al. (2005) precipitation (P), water vapor path (WVP), total surface heat flux, outgoing longwave radiation (OLR), day 50 of simulation.

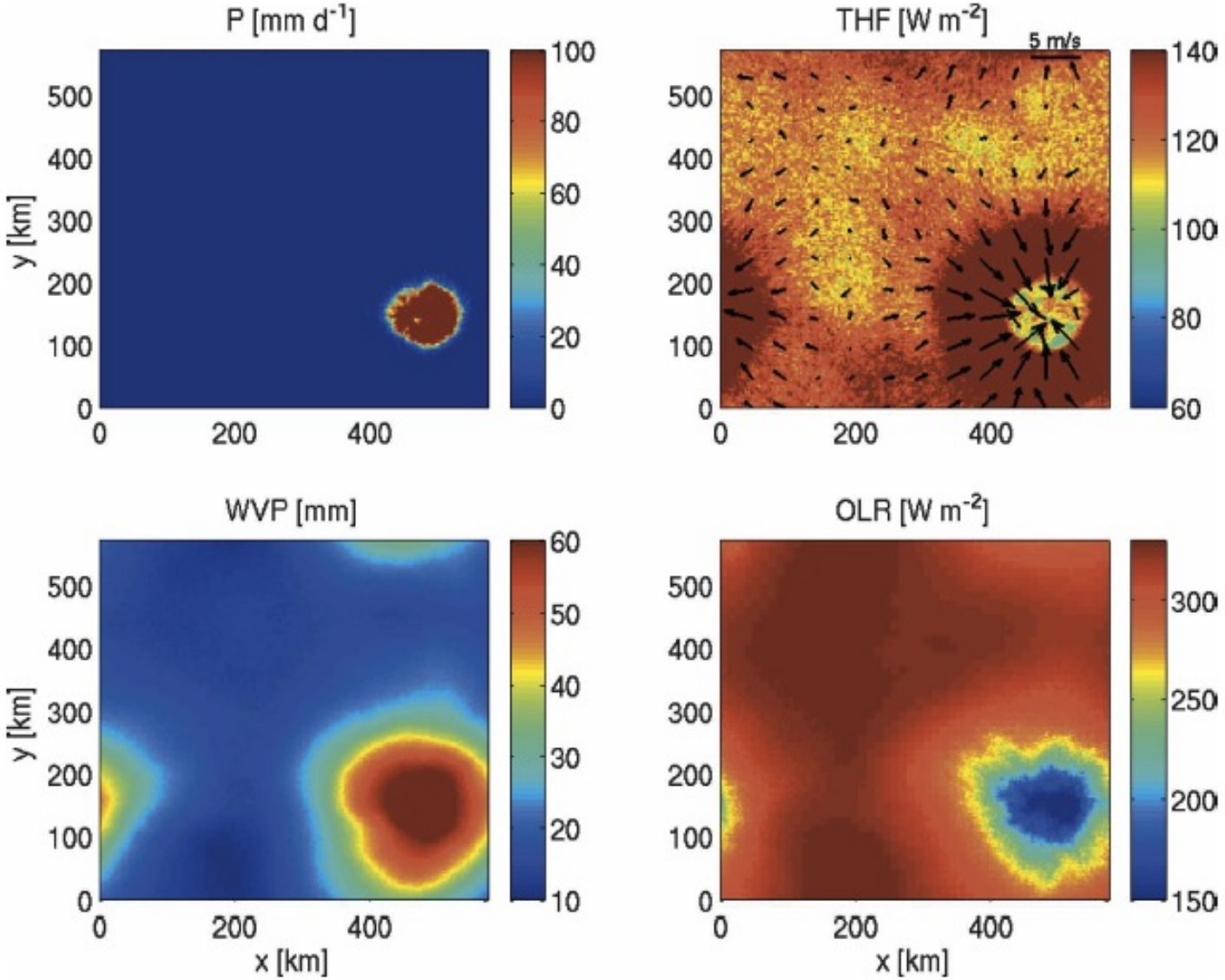

Self-aggregation - 2

Some notes on self-aggregation:

- It has now been reproduced a number of times with different models;
- It appears that interactions with surface fluxes and, especially, radiation are essential;
- We believe it is captured by SCM or CRM under WTG - the wet and dry regions are the multiple equilibria!
- If Coriolis is present, tropical cyclones form.

(e.g. Muller and Held 2012; Wing and Emanuel 2013)

WTG single column model, SST and free tropospheric temperature that allow steady deep convection; initialize with very dry troposphere and it persists

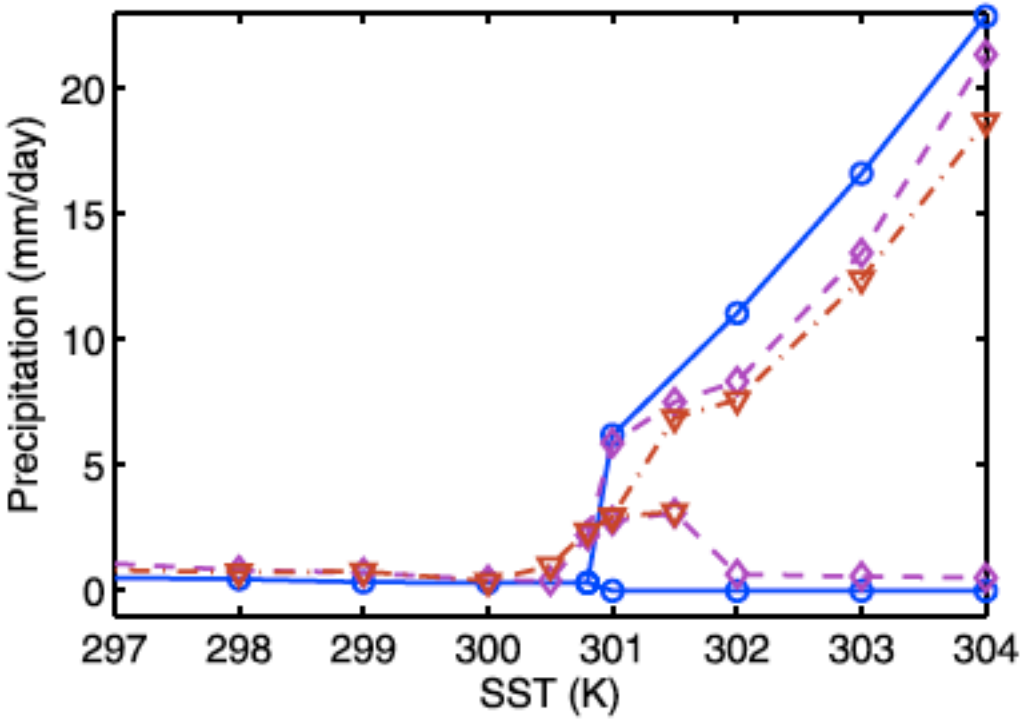

Sobel, Bellon and Bacmeister, *Geophys. Res. Lett.*, 2007

The same thing is found in a cloud-resolving model under WTG

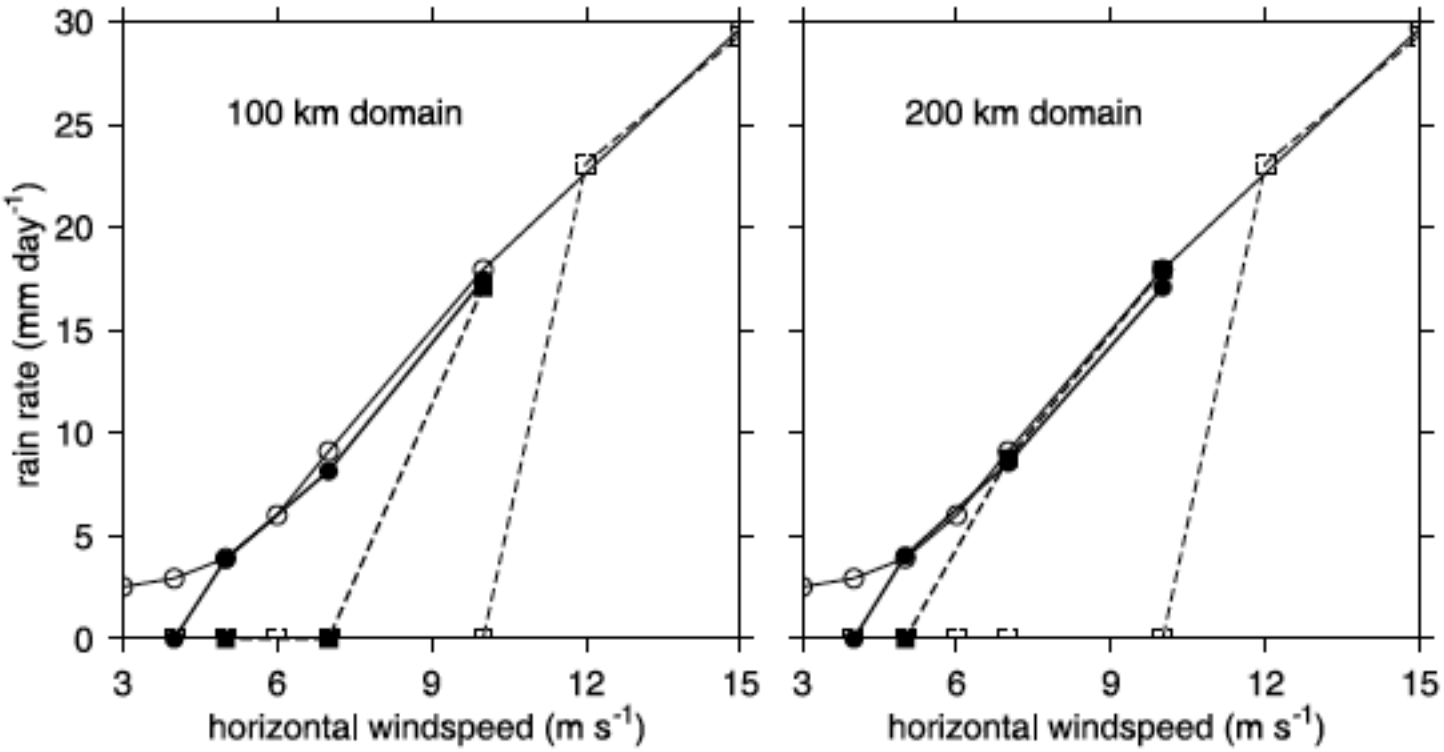

Sessions et al., *J. Geophys. Res.,* 2010; different symbols represent different simulation domain size

We believe these equilibria to be analogs to the rainy and dry parts of the domain under self-aggregation

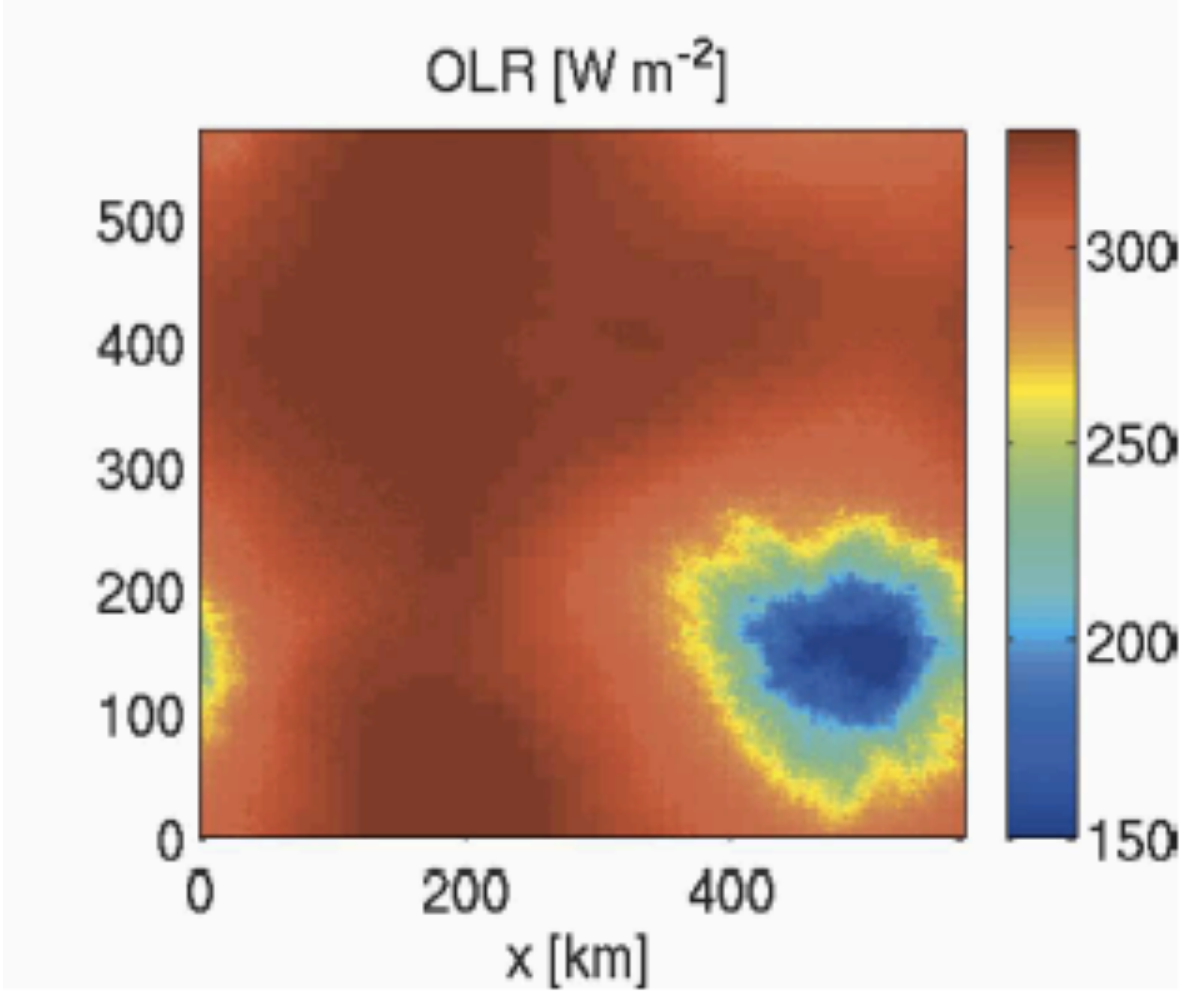

Bretherton et al. (2005)

Conserved variable budgets, 1

Following Neelin and Held (1987, *Mon. Wea. Rev.*, and Neelin and Zeng (2000), etc. We work with moist static energy, but could use entropy with little modification to the arguments.

$$\frac{\partial \overline{s}}{\partial t} + \overline{\mathbf{v}} \cdot \nabla \overline{s} + \overline{\omega} \frac{\partial \overline{s}}{\partial p} = Q_1 = Q_c + Q_R,$$

$$L_v \left(\frac{\partial \overline{q}}{\partial t} + \overline{\mathbf{v}} \cdot \nabla \overline{q} + \overline{\omega} \frac{\partial \overline{q}}{\partial p} \right) = -Q_2,$$

Drop overbars; everything is implicitly grid-scale. Add the equations to get a moist static energy equation:

$$\frac{\partial h}{\partial t} + \mathbf{v} \cdot \nabla h + \omega \frac{\partial h}{\partial p} = Q_c - Q_2 + Q_R.$$

Now integrate vertically between nominal (fixed) surface and tropopause pressures

$$\int_{p_T}^{p_0} \frac{\partial h}{\partial t} dp + \int_{p_T}^{p_0} \mathbf{v} \cdot \nabla h dp + \int_{p_T}^{p_0} \omega \frac{\partial h}{\partial p} dp = g(L_v E + H) + \int_{p_T}^{p_0} Q_R dp.$$

Conserved variable budgets, 2

Now assume that the vertical velocity has a known vertical structure which can be separated out:

$$\omega(x, y, p, t) = \Omega(p)\hat{\omega}(x, y, t).$$

Think of $\hat{\omega}$ as the vertical motion at a fixed level (e.g., 500 hPa). Then we can write

$$\int_{p_T}^{p_0} \frac{\partial h}{\partial t} dp + \int_{p_T}^{p_0} \mathbf{v} \cdot \nabla h dp + \hat{\omega} \int_{p_T}^{p_0} \Omega(p) \frac{\partial h}{\partial p} dp = g(L_v E + H) + \int_{p_T}^{p_0} Q_R dp.$$

or

$$\int_{p_T}^{p_0} \frac{\partial h}{\partial t} dp + \int_{p_T}^{p_0} \mathbf{v} \cdot \nabla h dp - \hat{\omega} M = g(L_v E + H) + \int_{p_T}^{p_0} Q_R dp,$$

where we have defined the **gross moist stability**

$$M = -\int_{p_T}^{p_0} \Omega(p) \frac{\partial h}{\partial p} dp.$$

Conserved variable budgets, 2

Analogously we can define the gross dry stability and gross moisture stratification

$$M_s = -\int_{p_T}^{p_0} \Omega(p) \frac{\partial s}{\partial p} dp,$$

$$M_q = \int_{p_T}^{p_0} \Omega(p) \frac{\partial q}{\partial p} dp,$$

so that $M = M_s - M_q$

Conserved variable budgets, 4

In steady state, if we can neglect the horizontal advection term, we can write the dry static energy budget

$$-g^{-1}\hat{\omega}M_s = L_v P + H - \int_{p_T}^{p_0} Q_R dp;$$

using that to substitute in for $\hat{\omega}$ in the MSE budget, and neglecting the sensible heat flux, we have

$$L_v P = \frac{M_s}{M}(L_v E + R) - R,$$

where $R = \int_{p_T}^{p_0} Q_R dp$.

Conserved variable budgets, 4

$$L_v P = \frac{M_s}{M}(L_v E + R) - R,$$

Strictly, all we have done is re-label things - this is formally just a diagnostic exercise. But **if we had a theory for the parameter M_s/M, this would be a predictive theory for steady-state precipitation in terms of the boundary fluxes**; R is the difference between surface and top-of atmosphere radiative fluxes, since radiative cooling is divergence of radiative flux.

Conserved variable budgets, 5

If the vertical motion profile $\Omega(p)$ were truly constant, then the gross moist stability would be a function of the h profile (mainly of the q profile, since the T profile $\sim$ constant in the tropics. This is what was assumed by Neelin and Held (1987, *Mon. Wea. Rev.*)

$$M = -\int_{p_T}^{p_0} \Omega(p) \frac{\partial h}{\partial p} dp.$$

But in reality, the vertical motion profile is variable, and probably has a stronger effect on variations in M.

Conserved variable budgets, 6

To think about the gross moist stability it is useful to integrate by parts

$$M = -\int_{p_T}^{p_0} \Omega(p) \frac{\partial h}{\partial p} dp = -[\Omega h] + \int_{p_T}^{p_0} \frac{d\Omega}{dp} h \; dp;$$

Since Ω is a vertical velocity we assume it to be zero at the boundaries (so first term vanishes) and by mass conservation note that it must have an associated horizontal velocity profile $V(p)$ such that

$$\frac{d\Omega(p)}{dp} \hat{\omega}(x, y, t) + V(p) \nabla \cdot \hat{\mathbf{v}}(x, y, t) = 0.$$

Then

$$M \sim \int_{p_T}^{p_0} Vh \; dp,$$

where V is the divergent wind.

Conserved variable budgets, 7

Putting the tendency and advection terms back, we can write the moist static energy equation as

$$\frac{\partial}{\partial t}\int_{p_T}^{p_0} h\ dp + \int_{p_T}^{p_0} \mathbf{v}\cdot\nabla h dp - \hat{\omega}M = g(L_v E + H) + R$$

where $R = \int_{p_T}^{p_0} Q_R dp$. We also assume that variations in water vapor are large compared to variations in temperature (or geopotential) so that

$$\frac{\partial}{\partial t}\int_{p_T}^{p_0} h\ dp \approx \frac{\partial}{\partial t}\int_{p_T}^{p_0} L_v q\ dp = \frac{\partial W}{\partial t},$$

where $W = \int_{p_T}^{p_0} L_v q\ dp$ is column water vapor (times l_v). Since moisture is mostly located in the lower troposphere, and large-scale winds tend to have "first baroclinic mode" structure where the winds are coherent (same sign) through the lower troposphere, it is reasonable to write the horizontal advection term in terms of some effective lower-tropospheric wind $\mathbf{V}$,

$$\int_{p_T}^{p_0} \mathbf{v}\cdot\nabla h\ dp \approx \mathbf{V}\cdot\nabla\int_{p_T}^{p_0} h\ dp \approx \mathbf{V}\cdot\nabla W.$$

Conserved variable budgets, 8

Thus our MSE equation is (absorbing all factors g, L_v into definitions of fluxes on RHS)

$$\frac{\partial W}{\partial t} + \mathbf{V} \cdot \nabla W = \hat{\omega} M + E + H + R.$$

Now we make the so-called **weak temperature gradient approximation** in the dry static energy equation, neglecting tendency and advection,

$$-\hat{\omega} M_s = P + H + R,$$

which we can use to eliminate $\hat{\omega}$ from the MSE equation

$$\frac{\partial W}{\partial t} + \mathbf{V} \cdot \nabla W = -\frac{M}{M_s}(P + H + R) + E + H + R;$$

or neglecting H compared to E and R (very good approximation over ocean),

$$\frac{\partial W}{\partial t} + \mathbf{V} \cdot \nabla W = -\frac{M}{M_s}(P + R) + E + R.$$

Conserved variable budgets, 9

$$\frac{\partial W}{\partial t} + \mathbf{V} \cdot \nabla W = -\frac{M}{M_s}(P + R) + E + R.$$

Some notes about this equation:

- The first term on the RHS is really a vertical advection term (though it doesn't look like it any more).
- We generally expect the factor $M/M_s < 1$; it may be $\ll 1$, or may even be negative in some circumstances. There is no a priori reason to treat it as constant, but neither is there any solid theory to justify any particular variations (and hard to constrain observationally).
- This would be a closed equation if we could express P, E, R, and $\mathbf{V}$ as functions of W (sounds difficult but ...).

Wang and Sobel (2011, *J. Geophys. Res.*)

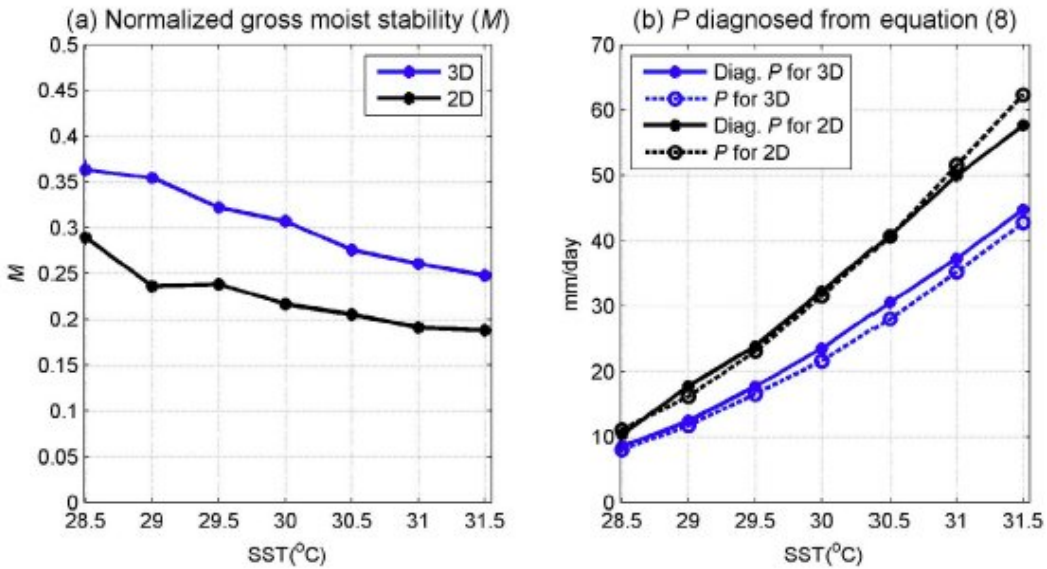

Sobel et al. (2004, *Mon. Wea. Rev.*)

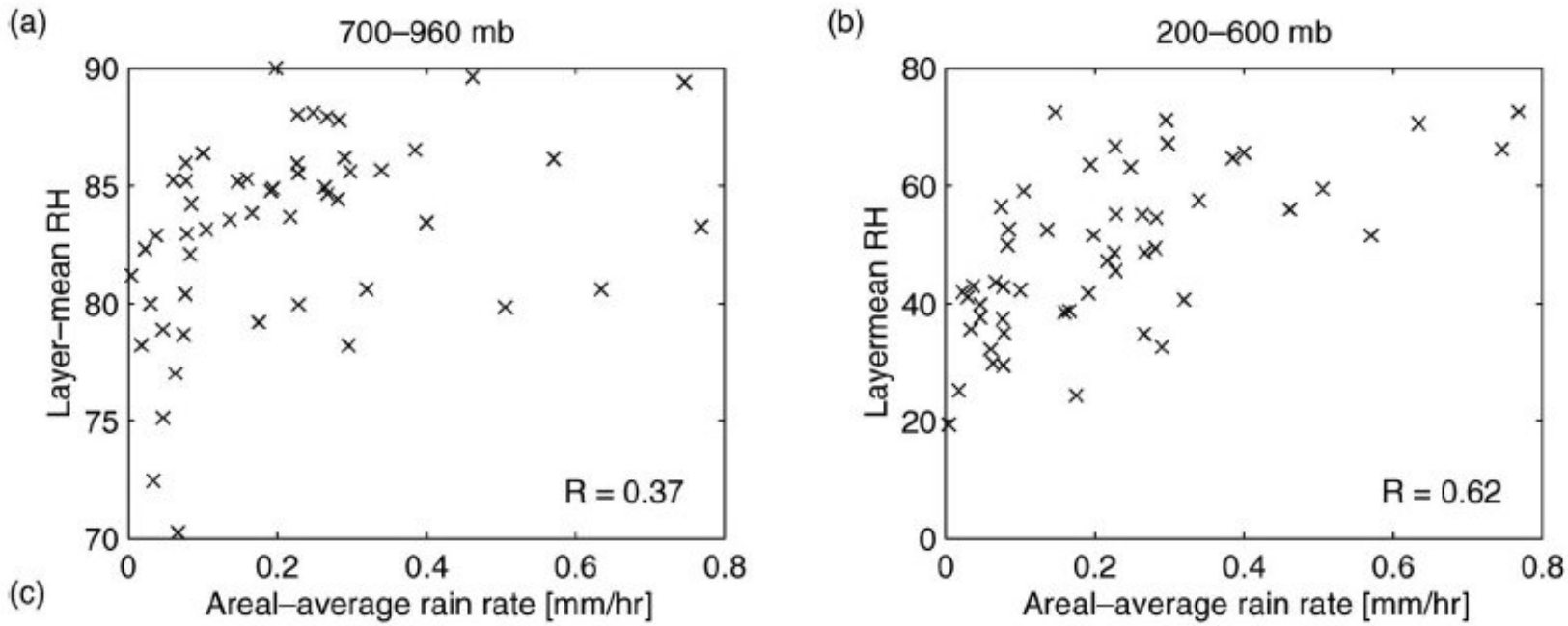

CAPE seems only weakly related to precipitation, while lower-tropospheric humidity seems a clearer causal factor (Sobel et al. 2004, *Mon. Wea. Rev.*)

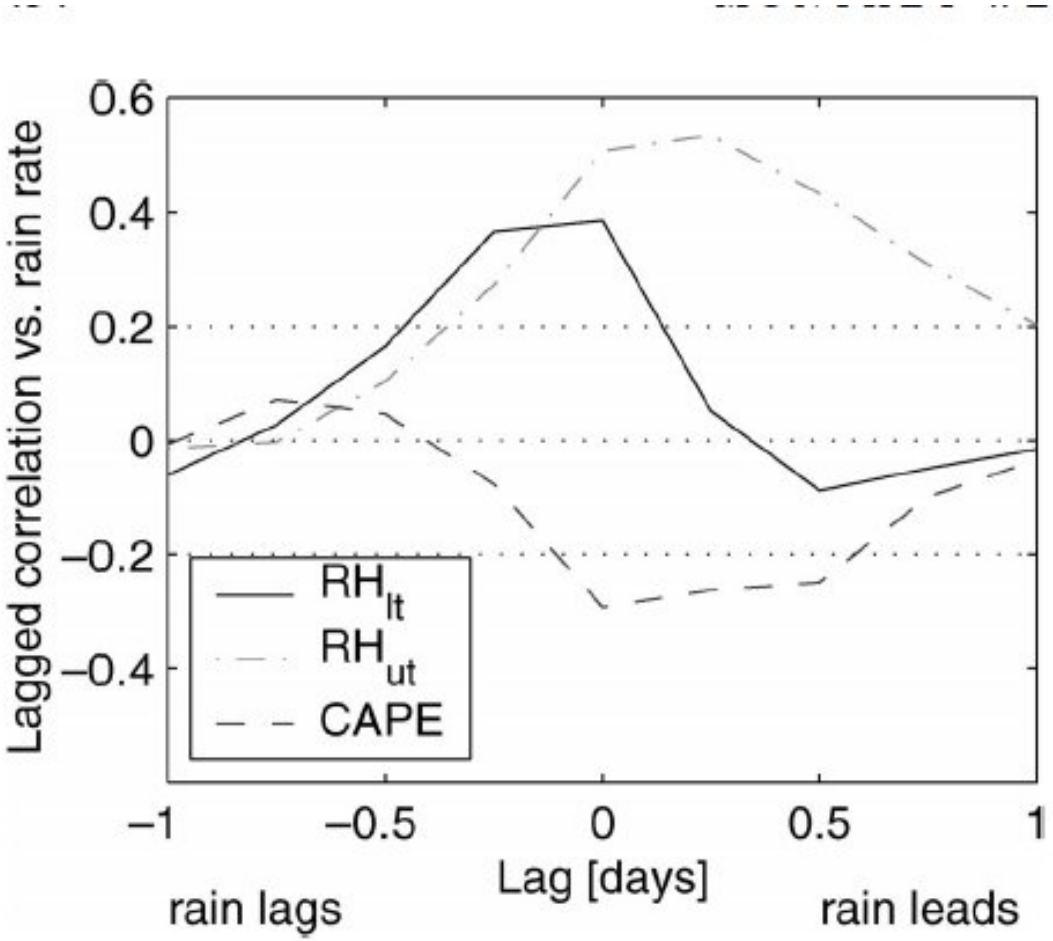

Wang and Sobel (2011, *J. Geophys. Res.*), instantaneous relationships between column water vapor and precipitation in a cloud resolving model under WTG.

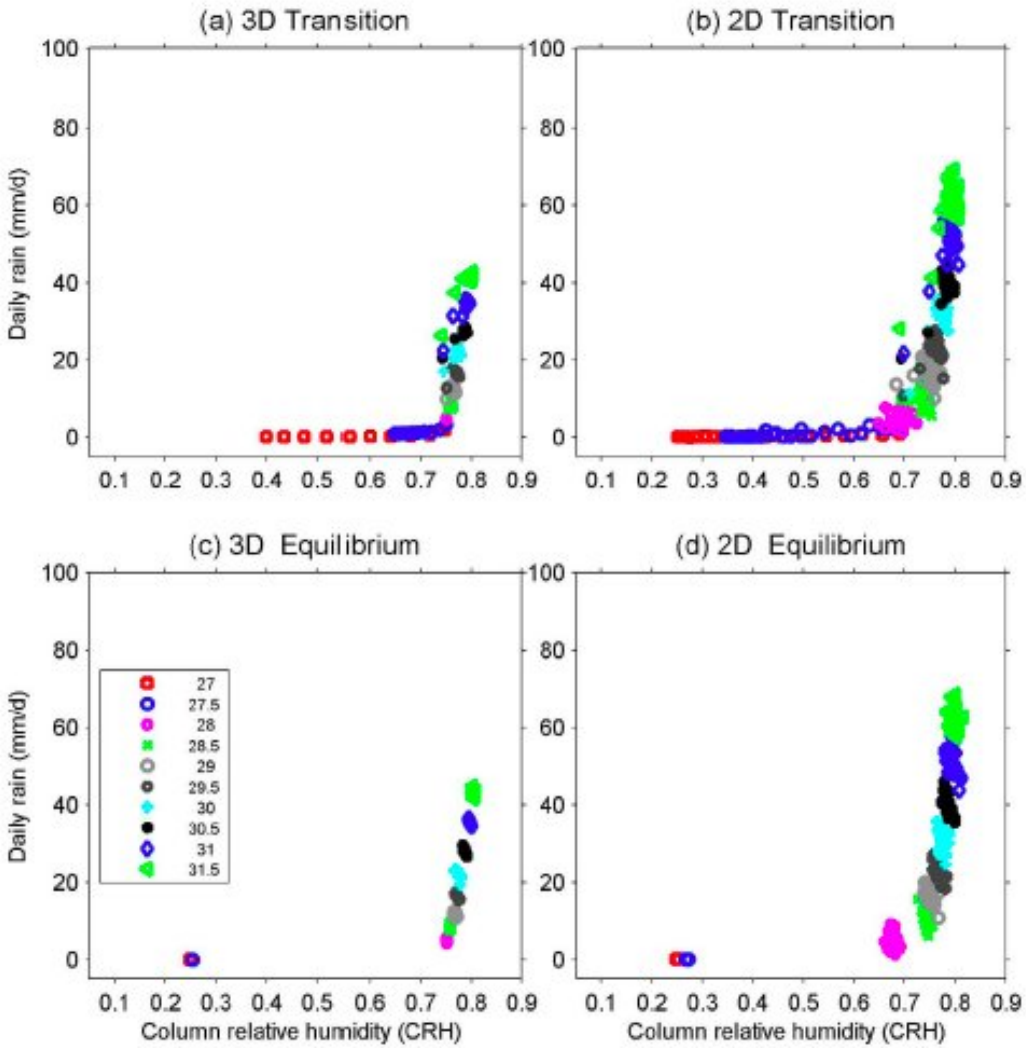

Bretherton et al. (2004) find an exponential relationship in satellite microwave observations.

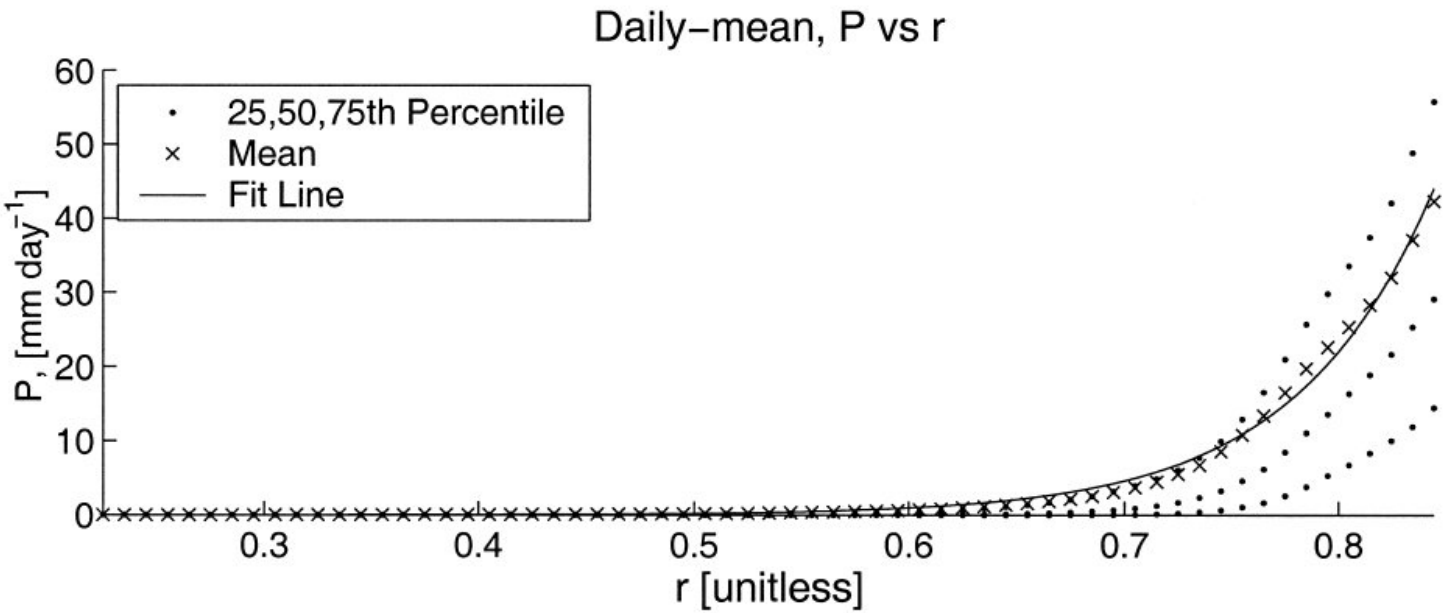

FIG. 4. Distribution of daily precipitation P in 1% bins of column-relative humidity r for all tropical ocean grid points in all months of 1998–2001. Dots show the 25th, 50th, and 75th percentiles of precipitation in each bin. The Xs show the bin-mean precipitation. The solid curve is the exponential fit (2).

Radiative cooling is also tightly coupled to precipitation, since OLR is. (E.g., Raymond et al. 2003, *J. Atmos. Sci.*)

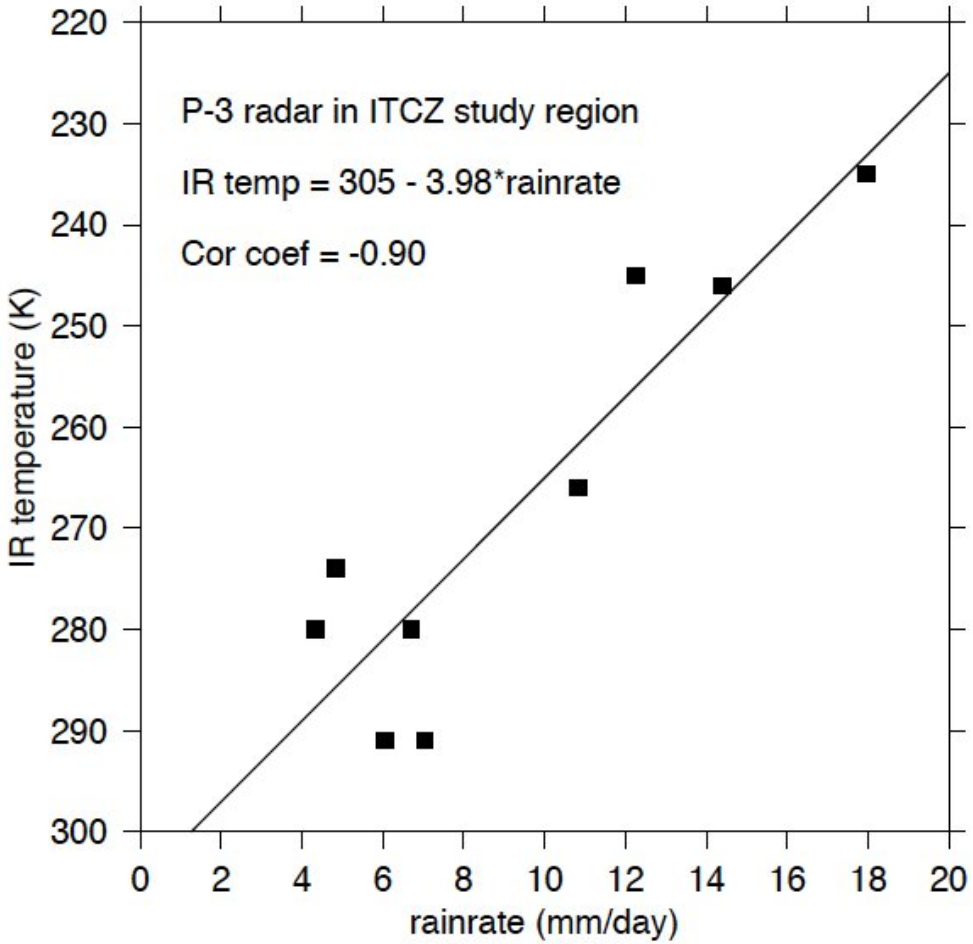

So, we argue that the following physical parameterizations may be adequate for the purposes of understanding some large-scale phenomena qualitatively (though not for serious numerical prediction):

$$P = P_0 \exp(\frac{W}{W^*}),$$

that is, precipitation a function (here exponential) of column relative humidity, and

$$R = R_0 + rP$$

that is, radiative heating increasing (or really, cooling decreasing, since the clear-sky radiative heating $R_0 < 0$) linearly with precipitation rate.

Reference1

- Bretherton, C. S., M. E. Peters, and L. E. Back, 2004: Relationships between Water Vapor Path and Precipitation over the Tropical Oceans. J. Clim., 17, 1517-1528
- Bretherton, C. S., P. N. Blossey, and M. Khairoutdinov, 2005: An Energy-Balance Analysis of Deep Convective Self-Aggregation above Uniform SST. J. Atmos. Sci., 62, 4273–4292
- Dunkerton, T. J., M. T. Montgomery, and Z. Wang, 2009: Tropical cyclogenesis in a tropical wave critical layer: easterly waves. Atmos. Chem. Phys., 9, 5587–5646
- Emanuel, K. A., 1987: An Air-Sea Interaction Model of Intraseasonal Oscillations in the Tropics. J. Atmos. Sci., 44, 2324–2340
- Emanuel, K. A., J. David Neelin, and C. S. Bretherton, 1994: On large-scale circulations in convecting atmospheres. Q. J. R. Meteorol. Soc., 120, 1111–1143
- Gill, A. E., 1980: Some simple solutions for heat-induced tropical circulation. Q. J. R. Meteorol. Soc., 106, 447–462

Reference2

- Kiladis, G. N., C. D. Thorncroft, and N. M. J. Hall, 2006: Three-Dimensional Structure and Dynamics of African Easterly Waves. Part I: Observations. J. Atmos. Sci., 63, 2212–2230
- Kiladis, G. N., M. C. Wheeler, P. T. Haertel, K. H. Straub, and P. E. Roundy, 2009: Convectively coupled equatorial waves. Rev. Geophys., 47, 1–42
- Lau, K.-H., and N.-C. Lau, 1990: Observed Structure and Propagation Characteristics of Tropical Summertime Synoptic Scale Disturbances. Mon. Weather Rev., 118, 1888–1913
- Matsuno, T., 1966: Quasi-Geostrophic Motions in the Equatorial Area. J. Meteorol. Soc. Japan, 44, 25–43
- Montgomery, M. T., L. L. Lussier III, R. W. Moore, and Z. Wang, 2010: The genesis of Typhoon Nuri as observed during the Tropical Cyclone Structure 2008 (TCS-08) field experiment – Part 1: The role of the easterly wave critical layer. Atmos. Chem. Phys., 10, 9879–9900
- Muller, C. J., and I. M. Held, 2012: Detailed Investigation of the Self-Aggregation of Convection in Cloud-Resolving Simulations. J. Atmos. Sci., 69, 2551–2565

Reference3

- Neelin, J. D., and I. M. Held, 1987: Modeling Tropical Convergence Based on the Moist Static Energy Budget. Mon. Weather Rev., 115, 3–12
- Neelin, J. D., and N. Zeng, 2000: A Quasi-Equilibrium Tropical Circulation Model—Formulation. J. Atmos. Sci., 57, 1741–176
- Neelin, J. D., I. M. Held, and K. H. Cook, 1987: Evaporation-Wind Feedback and Low-Frequency Variability in the Tropical Atmosphere. J. Atmos. Sci., 44, 2341–2348
- Raymond, D. J., G. B. Raga, C. S. Bretherton, J. Molinari, C. López-Carrillo, and Ž. Fuchs, 2003: Convective Forcing in the Intertropical Convergence Zone of the Eastern Pacific. J. Atmos. Sci., 60, 2064–2082
- Reed, R. J., and E. E. Recker, 1971: Structure and Properties of Synoptic-Scale Wave Disturbances in the Equatorial Western Pacific. J. Atmos. Sci., 28, 1117–1133
- Sessions, S. L., S. Sugaya, D. J. Raymond, and A. H. Sobel, 2010: Multiple equilibria in a cloud-resolving model using the weak temperature gradient approximation. J. Geophys. Res., 115, D12110

Reference4

- SOBEL, A. H., and C. S. BRETHERTON, 2003: Large-scale waves interacting with deep convection in idealized mesoscale model simulations. Tellus A, 55, 45–60
- Sobel, A. H., S. E. Yuter, C. S. Bretherton, and G. N. Kiladis, 2004: Large-Scale Meteorology and Deep Convection during TRMM KWAJEX. Mon. Weather Rev., 132, 422–444
- Sobel, A. H., G. Bellon, and J. Bacmeister, 2007: Multiple equilibria in a single-column model of the tropical atmosphere. Geophys. Res. Lett., 34, L22804
- Wang, S., and a. H. Sobel, 2011: Response of convection to relative sea surface temperature: Cloud-resolving simulations in two and three dimensions. J. Geophys. Res., 116, D11119
- Webster, P. J. P., 1972: Response of the tropical atmosphere to local, steady forcing. Mon. Weather Rev., 313, 518–541
- Wheeler, M., and G. N. Kiladis, 1999: Convectively Coupled Equatorial Waves: Analysis of Clouds and Temperature in the Wavenumber-Frequency Domain. J. Atmos. Sci., 56, 374–399

Reference5

- Wheeler, M., G. N. Kiladis, and P. J. Webster, 2000: Large-Scale Dynamical Fields Associated with Convectively Coupled Equatorial Waves. J. Atmos. Sci., 57, 613–640